Assessing trade-offs among electrification and grid decarbonization in a clean energy transition: Application to New York State

Supplementary Materials

Terence Conlon[a†*], Michael Waite[a†**], Yuezi Wu[a***], and Vijay Modi[a****]

[a]Department of Mechanical Engineering, Columbia University
220 S.W. Mudd Building, 500 West 120th Street, New York, NY 10027, USA

[†] Corresponding author
* tmc2180@columbia.edu
** mbw2113@columbia.edu
*** yw3054@columbia.edu
**** modi@columbia.edu

Table of Contents

S1 Supplementary Nomenclature

Additional fixed variables and parameters

C_{fuel}	total fuel cost for fossil fuel-based generation over entire analysis period [$]
$CAP_{h2-e,i}$	hydrogen storage energy capital cost at node *i* [$/MWh]
$CAP_{h2-p,i}$	hydrogen storage power capital cost at node *i* [$/MW]
$D^{t}_{veh-fix,i}$	vehicle fixed charging demand at node *i* [MWh]
$E^{daily}_{veh,i}$	daily vehicle charging demand at node *i* [MWh]
$E^{daily}_{veh-fix,i}$	daily vehicle fixed charging demand at node *i* [MWh]
$E^{daily}_{veh-flex,i}$	daily vehicle flexible charging demand at node *i* [MWh]
$E^{daily}_{veh-tot,i}$	total daily vehicle charging demand at node *i* (fixed plus flexible) [MWh]
f_{c-s}	cubic spline function
$h_{veh-start}$	electric vehicle charging start time
$h_{veh-end}$	electric vehicle charging end time
$h_{veh-min}$	minimum number of hours required for full daily electric vehicle charging [hours]
$H^{daily}_{flex,i}$	daily flexible hydropower generation at node *i* [MWh]
$H^{monthly}_{fix,i}$	monthly fixed hydropower generation at node *i* [MWh]
$H^{monthly}_{flex,i}$	monthly flexible hydropower generation at node *i* [MWh]
$H^{monthly}_{tot,i}$	monthly total hydropower electricity generation at node *i* (fixed plus flexible) [MWh]
L^{daily}_{i}	daily biofuel generation at node *i* [MWh]
L^{max}_{i}	biofuel maximum generation at node *i* [MWh]
m	day index
omf_{h2}	hydrogen storage fixed operations and management cost [$/MW-yr]
V^{max}_{i}	maximum hourly electricity import limit at node *i* [MWh]
$X^{existing}_{batt-e,i}$	capacity of existing battery energy at node *i* [MWh]
$X^{existing}_{batt-p,i}$	capacity of existing battery power at node *i* [MW]
$X^{existing}_{bio,i}$	capacity of existing biofuel generation at node *i* [MW]
$X^{existing}_{ff,i}$	capacity of existing fossil fuel-based generation at node *i* [MW]
$X^{existing}_{hydro,i}$	capacity of existing hydropower generation at node *i* [MW]
$X^{existing}_{nuc,i}$	capacity of existing nuclear generation at node i [MW]
$X^{existing}_{tx,ii'}$	capacity of existing transmission between node *i* and adjacent node *i'* [MW]
y	fraction
η_{batt}	one-way battery storage efficiency
η_{h2}	one-way hydrogen storage efficiency
η_{veh}	electric vehicle charging efficiency
κ	storage self-discharge
σ	fossil fuel-based generation reserve requirement

$\varphi_{p2e-batt-min}$ minimum possible battery storage power-to-energy ratio
$\varphi_{p2e-batt-max}$ maximum possible battery storage power-to-energy ratio
$\varphi_{p2e-h2-min}$ minimum possible hydrogen storage power-to-energy ratio
$\varphi_{p2e-h2-max}$ maximum possible hydrogen storage power-to-energy ratio

Additional decision variables
All variables are constrained to be greater than or equal to 0.

$D^t_{veh-flex,i}$ hourly vehicle flexible charging demand at node *i* [MWh]
$E^t_{batt,i}$ aggregate battery storage state of charge at node *i* and timestep *t* [MWh]

$E^t_{h2,i}$ aggregate hydrogen storage state of charge at node *i* [MWh]
$X_{h2-e,i}$ hydrogen storage energy capacity installed at node *i* [MWh]
$X_{h2-p,i}$ hydrogen storage power capacity installed at node *i* [MW]
$\gamma^t_{h2,i}$ increase in hydrogen storage state of charge at node *i* [MWh]
$\delta^t_{h2,i}$ decrease in hydrogen storage state of charge at node *i* [MWh]

Additional scenario configuration parameters

RGT renewable electricity generation target: Fraction of total demand that must be met by renewable energy (combined wind, water, and solar power)

Additional subscripts and superscripts

gas motor gasoline
h2 hydrogen storage
max maximum
ng natural gas

S2 Supplementary Methodology

Section S2 presents the remainder of methodology for the System Electrification and Capacity TRansition (SECTR) framework, and how the framework is applied to the New York State (NYS) energy system (SECTR-NY).

S2.1 Remainder of general formulation governing equations

The following sections contain the governing equations for the SECTR general formulation not specified in Section 2.1 of the main text.

Characterization of fossil fuel generation

Fossil fuel-based electricity generation from existing, $X_{ff,i}^{existing}$, and new, $X_{ff,i}$, capacity is modeled. In scenarios where $X_{ff,i}$ is selected, all new generation is provided by simple cycle gas turbines, because of the very low load factors of peak load increases with heating and vehicle electrification [1]. Existing fossil fuel-based generation efficiency, $\eta_{ff-existing}$, is determined from historical data; new gas turbine efficiency, η_{ff-new}, is based on advanced combustion turbines [2]. Fossil fuel generation costs are computed per Eq. (S1).

$$C_{fuel} = \sum_{t \in T} \sum_{i \in I} 3.412 * c_{ff,i} * \left(\frac{G_{existing,i}^{t}}{\eta_{ff-existing}} + \frac{G_{new,i}^{t}}{\eta_{ff-new}} \right) \tag{S1}$$

A capacity reserve margin on $X_{ff,i}^{existing}$ and $X_{ff,i}$ is also imposed:

$$X_{ff,i}^{existing} \geq (1 + \sigma) * G_{existing,i}^{t} \tag{S2}$$

$$X_{ff,i} \geq (1 + \sigma) * G_{new,i}^{t} \tag{S3}$$

To avoid significant increases in computation time, fossil fuel-based generation start-up costs are linearized as ramping costs, $c_{ff-ramp}$, on a per-MW per-hour basis ($/MW-h); this quantity is applied to $G_{new-diff,i}^{t}$ and $G_{existing-diff,i}^{t}$, variables which represent the absolute value of the hourly change in gas generation (Eqs. (S4-S5)). Ramping limitations are not imposed on the gas generators [3].

$$G_{existing-diff,i}^{t} = | G_{existing,i}^{t} - G_{existing,i}^{t-1} | \tag{S4}$$

$$G^{t}_{new-diff,i} = \mid G^{t}_{new,i} - \ G^{t-1}_{new,i} \mid$$

(S5)

Wind capacity

Both new onshore, $X_{on,i}$, and offshore, $X_{off,i}$, wind capacities are simulated, and are limited by resource availability and maximum capacity available at each node (onshore, Eq. (S6)) or within the study region (offshore, Eq. (S7)):

$$X^{existing}_{on,i} + X_{on,i} \ \leq X^{max}_{on,i}$$

(S6)

$$\sum_{i \in I} \left(X^{existing}_{off,i} + \ X_{off,i} \right) \leq X^{max}_{off}$$

(S7)

Solar capacity

Node-specific BTM solar capacity, $X_{btm-solar,i}$, produces fixed generation at each node equal to the product of user-imposed capacity and the supplied generation potential time series, $W^{t}_{btm-solar,i}$. BTM solar is treated as must-run.

Utility-scale solar capacity is constrained per Eq. (S8):

$$X^{existing}_{us-solar,i} + X_{us-solar,i} \ \leq X^{max}_{us-solar,i}$$

(S8)

Internodal transmission

The cost of maintaining existing transmission capacity is based on user inputs for historical transmission costs and flows. Costs of new transmission capacity are defined for each internodal interface. Transmission losses of 3% between adjacent nodes are assumed, and a nominal cost of transmission ($0.01/MWh) is applied. Eq. (S9) limits internodal transmission flow, $Z^{t}_{ii'}$, to the combined capacity of existing, $X^{existing}_{tx,ii'}$,and new, $X_{tx,ii'}$, transmission:

$$Z^{t}_{ii'} \ \leq X^{existing}_{tx,ii'} + X_{tx,ii'}$$

(S9)

Battery storage

Energy storage is based on lithium-ion batteries and is modeled as bulk storage at each node. Modeled batteries are constrained to a power-to-energy ratio, $\varphi_{p2e-batt}$, and a single efficiency, η_{batt}, applied on both charge and discharge. A nominal \$0.01/MWh cost is attached to battery charge, $\gamma^t_{batt,i}$, and discharge, $\delta^t_{batt,i}$; storage self-discharge, κ, is also included. Battery storage constraints are presented in Eqs. (S10-S14).

$$\frac{\delta^t_{batt,i}}{\eta_{batt}} - \eta_{batt} * \gamma^t_{batt,i} = (1-\kappa) * E^T_{batt,i} - E^t_{batt,i} \ , \qquad \forall t = 0 \tag{S10a}$$

$$\frac{\delta^t_{batt,i}}{\eta_{batt}} - \eta_{batt} * \gamma^t_{batt,i} = (1-\kappa) * E^{t-1}_{batt,i} - E^t_{batt,i} \ , \qquad \forall t > 0 \tag{S10b}$$

$$E^t_{batt,i} \leq X_{batt-e,i} + X^{existing}_{batt-e,i} \tag{S11}$$

$$\gamma^t_{batt,i} \leq X_{batt-p,i} + X^{existing}_{batt-p,i} \tag{S12}$$

$$\delta^t_{batt,i} \leq X_{batt-p,i} + X^{existing}_{batt-p,i} \tag{S13}$$

$$\varphi_{p2e-batt-min} * (X_{batt-p,i} + X^{existing}_{batt-p,i}) \leq X_{batt-e,i} + X^{existing}_{batt-e,i} \leq \varphi_{p2e-batt-max} * (X_{batt-p,i} + X^{existing}_{batt-p,i}) \tag{S14}$$

In the SECTR formulation, storage self-discharge and nominal storage charge and discharge costs are included to limit the number of unique model solutions, thereby allowing the model to find an optimal solution more quickly. In the case where excess low-carbon generation is available over a period of hours, storage self-discharge reduces the number of ways to fully charge the storage to a single, unique schedule. As storage technologies undergo self-discharge in reality, the self-discharge parameter better allows SECTR to simulate likely battery operation. Moreover, when excess low-carbon generation is available and battery storage is fully charged, without nominal storage charge and discharge costs, nothing prevents the model from discharging the batteries, curtailing that energy, and then using the excess generation to recharge the batteries. Nominal charge and discharge costs prevent this type of unnecessary operation.

Nuclear generation

Nodal nuclear generation, N_i^t is modeled as constant based on a user input value and is treated as must-run.

Hydropower generation

SECTR includes modules for both fixed and flexible hydropower operation per [4]. Monthly hydropower generation is split into fixed, $H_{fix,i}^{monthly}$, and flexible, $H_{flex,i}^{monthly}$ quantities based on the nodal fraction of hydropower to be considered fixed, $y_{fix,i}$, as shown in Eqs. (S15-S16); both monthly generation quantities are fit with cubic splines, f_{c-s}, per Eqs. (S17-S18):

$$H_{fix,i}^{monthly} = y_{fix,i} * H_{tot,i}^{monthly} \tag{S15}$$

$$H_{flex,i}^{monthly} = (1 - y_{fix,i}) * H_{tot,i}^{monthly} \tag{S16}$$

$$H_{fix,i}^{t} = f_{c-s}(H_{fix,i}^{monthly}) \tag{S17}$$

$$H_{flex,i}^{daily} = f_{c-s}(H_{flex,i}^{monthly}) \tag{S18}$$

While fixed hydropower generation time series, $H_{fix,i}^t$, are treated as must-run, flexible hydropower generation, $H_{flex,i}^t$, can vary throughout the day to meet a daily nodal total, $H_{flex,i}^{daily}$, per Eqs. (S19-S20).

$$\sum_{t=1+24m}^{24*(m+1)} H_{flex,i}^{t} = H_{flex,i}^{daily}, \qquad m = 0..\frac{T}{24} - 1 \tag{S19}$$

$$H_{flex,i}^{t} \leq H_{flex,i}^{max} \tag{S20}$$

Biofuel generation

Biofuel generation, L_i^t, is assumed to have flexible operation, and can meet up to a set amount of daily generation, L_i^{daily}, without exceeding a nodal limit, L_i^{max}, at any time step per Eqs. (S21-S22):

$$\sum_{t=1+24m}^{24*(m+1)} L_i^t \leq L_i^{daily}, \qquad m = 0..\frac{T}{24} - 1 \tag{S21}$$

$$L_i^t \leq L_i^{max} \tag{S22}$$

Interregional imports

Electricity imports into the study region, V_i^t, are allowed at each node. All interregional imports are subject to a maximum limit, V_i^{max}, per Eq. (S23).

$$V_i^t \leq V_i^{max} \tag{S23}$$

Existing generation capacity costs

A fixed cost, $EX_{cap,i}$, is applied to eligible existing generation capacity, $X_{cap,i}^{existing}$, per Eq. (4) in the main text. All existing hydropower, nuclear, fossil-fuel, and biofuel capacity is included in this approach, per Eq. (S24).

$$X_{cap,i}^{existing} = X_{hydro,i}^{existing} + X_{nuc,i}^{existing} + X_{gt,i}^{existing} + X_{bio,i}^{existing} \tag{S24}$$

S2.2 Model Framework Additional Modeling Capabilities

The SECTR framework has additional modeling capabilities not used in any of the SECTR-NY results presented in the Main Text. These capabilities are detailed in the following paragraphs.

Objective function

With the inclusion of hydrogen storage energy and power capacity as SECTR decision variables, the total cost of new capacity is presented in Supplementary Eq. (S25):

$$C_{new-cap} = n_{years} * \sum_{i \in I} \Big[(A_{P_{on},j} * CAP_{on,i} + omf_{on}) * X_{on,i} + (A_{P_{off},j} * CAP_{off,i} + omf_{off}) * X_{off,i} + (A_{P_{us-solar},j} * CAP_{us-solar,i} + omf_{us-solar}) * X_{us-solar,i} + (A_{P_{batt},j} * CAP_{batt-e,i}) * X_{batt-e,i} + (A_{P_{batt},j} * CAP_{batt-p,i}) * X_{batt-p,i} + (A_{P_{h2},j} * CAP_{h2-e,i} + omf_{h2}) * X_{h2-e,i} + (A_{P_{h2},j} * CAP_{h2-p,i}) * X_{h2-p,i} + (A_{P_{ff},j} * CAP_{ff,i} + omf_{ff}) * X_{ff,i} + \sum_{i'} (A_{P_{tx},j} * CAP_{tx,ii'} * d_{ii'} + omf_{tx,ii'}) * X_{tx,ii'} \Big] \quad \text{(S25)}$$

The second SECTR objective function minimizes the levelized cost of electricity (LCOE) according to Supplementary Eq. (S26), where LCOE is defined in Eq. (5) of the main text. When this second objective function is applied, the user specifies a greenhouse gas (GHG) emission reduction, and SECTR determines the combination of low-carbon electricity percent (LCP) and heating and vehicle electrification rate (HVE) that allows for the lowest LCOE.

$$obj_2 = minimize(LCOE) \quad \text{(S26)}$$

Energy balance constraint

With the inclusion of hydrogen storage charge and discharge capabilities, nodal energy balance is constrained per Supplementary Eq. (S27):

$$(X_{on,i} + X_{on,i}^{existing}) * W_{on,i}^t + (X_{off,i} + X_{off,i}^{existing}) * W_{off,i}^t + (X_{us-solar,i} + X_{us-solar,i}^{existing}) * W_{us-solar,i}^t + X_{btm-solar,i} * W_{btm-solar,i}^t + H_{flex,i}^t + H_{fixed,i}^t + N_i^t + G_{existing,i}^t + G_{new,i}^t + L_i^t + V_i^t - \gamma_{batt,i}^t + \delta_{batt,i}^t - \gamma_{h2,i}^t + \delta_{h2,i}^t + \sum_{i'} [(1-l) * Z_{i'i}^t - Z_{ii'}^t] \geq \mathrm{D}_{elec,i}^t + \mathrm{D}_{heat,i}^t + D_{veh,i}^t \quad \text{(S27)}$$

Renewable electricity generation targets

In SECTR simulations, users can also select a renewable generation target (RGT) – a minimum percentage of electricity from onshore and offshore wind, hydropower, and solar. Accordingly,

the maximum allowable electricity generated from fossil fuels, biofuels, and nuclear power over the full simulation period is constrained per Supplementary Eq. (S28).

$$\sum_{t\in T}\sum_{i\in I}\left(G^t_{existing,i} + G^t_{new,i} + L^t_i + N^t_i\right) \leq (1 - RGT) * \sum_{t\in T}\sum_{i\in I}\left[\mathrm{D}^t_{elec,i} + \mathrm{D}^t_{heat,i} + D_{ev,i} - V^t_i - X_{btm-solar,i} * W^t_{btm-solar,i}\right] \quad \text{(S28)}$$

Flexible charging of electrified vehicle demand

SECTR includes another formulation for electric vehicle charging in which $\mathrm{D}^t_{veh,i}$ can be computed as the sum of a fixed electric vehicle demand, $D^t_{veh-fix,i}$, and a flexible electric vehicle demand, $D^t_{veh-flex,i}$, per Supplementary Eq. (S29):

$$\mathrm{D}^t_{veh,i} = D^t_{veh-fix,i} + D^t_{veh-flex,i} \quad \text{(S29)}$$

This formulation uses a daily nodal vehicle electricity requirement, $E^{daily}_{veh,i}$, calculated as the product of the nodal percentage of vehicle electrification (user-defined or computed, depending on model configuration), $p_{veh,i}$, and user-provided daily nodal electricity requirement for full vehicle electrification, $E^{daily,full}_{veh,i}$, per Supplementary Eq. (S30).

$$E^{daily}_{veh,i} = p_{veh,i} * E^{daily,full}_{veh,i} \quad \text{(S30)}$$

Here, SECTR allows flexibility in meeting daily vehicle electrification energy requirements. Users can split daily vehicle electricity energy demand, $E^{daily}_{veh,i}$, into flexible, $E^{daily}_{veh-flex,i}$, and fixed, $E^{daily}_{veh-fix,i}$, portions based on a provided fraction of daily vehicle electricity requirement allowed to be flexible, $y_{veh-flex}$, as shown in Supplementary Eqs. (S31-S32).

$$E^{daily}_{veh-flex,i} = y_{veh-flex} * E^{daily}_{veh,i} \quad \text{(S31)}$$

$$E^{daily}_{veh-fix,i} = (1 - y_{veh-flex}) * E^{daily}_{veh,i} \quad \text{(S32)}$$

In determining hourly flexible vehicle charging demand, $D^t_{veh-flex,i}$, SECTR requires that the user provide a timestep for the hour at which daily charging can start, $h_{veh-start}$ and a timestep indicating the last hour at which charging is allowed, $h_{veh-end}$. The standard SECTR formulation

establishes a lower limit of 4 hours, $h_{veh-min}$, for full daily flexible EV charging. The flexible vehicle charging and power constraints are shown below:

$$\sum_{t=\ h_{veh-start}}^{h_{veh-end}} D^t_{veh-flex,i} = \frac{E^{daily}_{veh-flex,i}}{\eta_{veh}}\ , \qquad for\ m = 0..\frac{T}{24} - 1 \tag{S33}$$

$$D^t_{veh-flex,i}\ \leq \frac{E^{daily}_{veh-flex,i}}{h_{veh-min}} \tag{S34}$$

To determine the hourly fixed vehicle charging demand, $D^t_{veh-fix,i}$, the daily fixed vehicle charging load is split equally across the same charging period. The fixed charging constraint is shown in Supplementary Eq. (S35).

$$D^t_{veh-fix,i} = \frac{E^{daily}_{veh-fix,i}}{\eta_{veh} * (h_{veh-end} - h_{veh-start} + 1)}\ , for\ t = (h_{veh-start} + 24m)\,..\,(h_{veh-end} + 24m),\ for\ m = \ 0..\frac{T}{24} - 1 \tag{S35}$$

Hydrogen storage

Long-term energy storage capabilities are modeled based on potential future system costs of grid-scale power-to-gas (P2G) with hydrogen (H2) gas: H2 produced by electrolysis, $\gamma^t_{h2,i}$; availability of a low-cost gas storage reservoir, $E^t_{h2,i}$; and electricity generated by H2 combustion in a gas turbine, $\delta^t_{h2,i}$. Nodal per-unit power capacity, $CAP_{h2-p,i}$, and energy capacity, $CAP_{h2-e,i}$, cost components are assigned. Hydrogen storage efficiency, η_{h2}, is applied on both charge and discharge. A self-discharge rate, κ, is also included.

SECTR places no constraints on the hydrogen storage power-to-energy ratio. Hydrogen storage energy balance, $E^t_{h2,i}$; power capacity, $X_{h2-p,i}$; energy capacity, $X_{h2-e,i}$; charging, $\gamma^t_{h2,i}$; and discharging, $\delta^t_{h2,i}$, constraints are shown in Supplementary Eqs. (S36-S39).

$$\frac{\delta^t_{h2,i}}{\eta_{h2}} - \ \eta_{h2} * \gamma^t_{h2,i} = (1-\kappa) * E^T_{h2,i} - E^t_{h2,i}\ , \qquad \forall t = 0 \tag{S36a}$$

$$\frac{\delta^t_{h2,i}}{\eta_{h2}} - \ \eta_{h2} * \gamma^t_{h2,i} = (1-\kappa) * E^{t-1}_{h2,i} - E^t_{h2,i}\ , \qquad \forall t > 0$$

(S36b)

$$E_{h2,i}^{t} \leq X_{h2-e,i}$$

(S37)

$$\gamma_{h2,i}^{t} \leq X_{h2-p,i}$$

(S38)

$$\delta_{h2,i}^{t} \leq X_{h2-p,i}$$

(S39)

Identical to the treatment of battery storage, hydrogen storage self-discharge and nominal charging and discharging costs are included to limit the number of unique model solutions for a given SECTR configuration.

S2.3 Application of the System Electrification and Capacity TRansition framework to New York State

The subsections below detail the SECTR-NY parameterization, including descriptions of all data sources used and model data development. In SECTR-NY, New York State (NYS) is split into four nodes based on the major transmission interfaces of the New York Independent System Operator (NYISO) control area; these nodes are shown in Supplementary Figure S1.

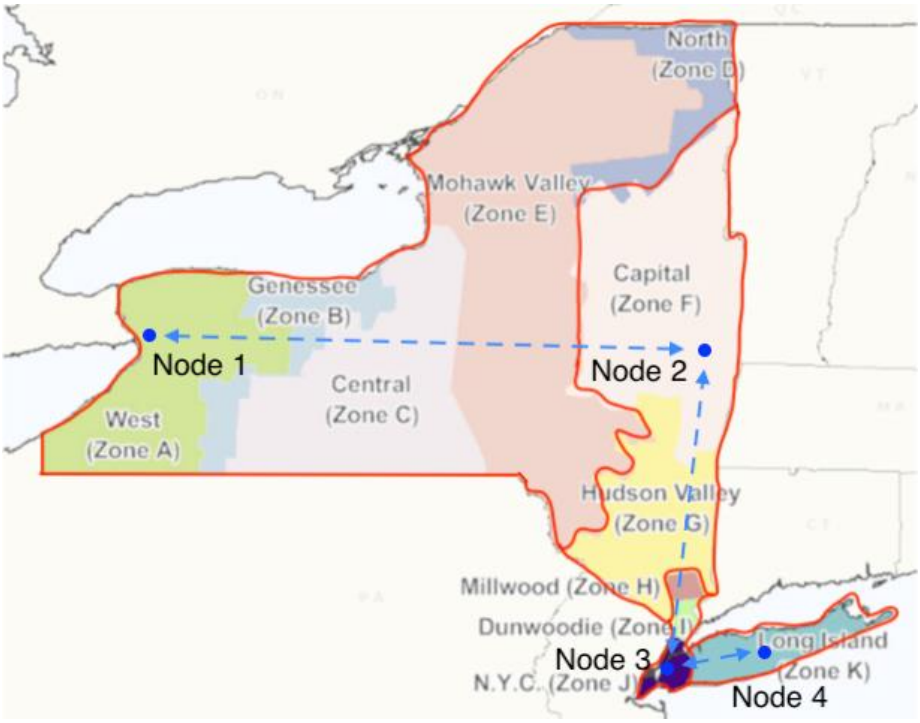

Supplementary Figure S1: NYISO control area load zones split into model nodes. Node boundaries and connections by authors; underlying image taken from [5].

In all simulations, low cost estimates are adopted for the technologies with multiple estimates available. All new generation technologies are annualized with a 20-year annualization period; all storage technologies are annualized with a 10-year annualization period. All model constraints presented in the Main Text that contain variables with nodal indexing are applied over all nodes in the study region; constraints which contain variables with temporal indexing are applied over all timesteps in the study period.

Nodal electricity demands

The existing electricity demand used is the 2007-2012 demand in each NYISO load zone [6], aggregated at each node per Supplementary Figure S1; the average existing statewide demand is 18,655 MWh/h. Supplementary Table S1 shows average and peak electricity demands at each node. Current electricity demands include some amount of electricity usage for heating and very limited use for passenger vehicles. Here, new electricity demands from converting current fossil

fuel end uses in buildings and on-road vehicles to electric technologies are also considered. (As discussed in the Main Text, fossil fuel end uses in buildings are thermal and dominated by space heating, "heating" is used for short.)

Nodal electricity demands for heating fossil fuel conversion to electric heat pumps (EHPs) are based on a nationwide building heating model described in detail in a recently published paper [7] and applied to 2007-2012 temperature data [8]. To convert fossil fuel demands to thermal loads, current average fossil fuel equipment efficiencies of 82% for space heating and 58% for DHW are assumed based on average values for "Installed Base" equipment from the US Energy Information Administration (EIA) [9]. The temperature-dependent coefficient of performance (COP) of new EHPs is based on the 90th percentile performance of EHPs in a regularly updated database of "cold climate" EHPs [10] and modeled per [8]. The COP of domestic hot water (DHW) EHPs was assumed to be a constant 2.32 based on the highest field-validated product performance from an National Renewable Energy Laboratory (NREL) study [11]. Full heating electrification results in a computed statewide average additional electricity load of 7573 MWh/h; however, the conversion of existing electric resistance heating to EHPs is also considered, which reduces statewide average heating electricity demand to 6716 MWh/h. Regional and statewide computed average and peak electrified heating values are shown in Supplementary Table S1.

To parameterize potential electric vehicle charging demand, the total 2018 volumetric sales of gasoline and diesel to New York transportation customers [12] are converted to miles driven using an assumed 21.0 miles per gallon (mpg). The latter assumption is based on an average vehicle age of 11.8 years in 2019 per the Bureau of Transportation Statistics [13] and the corresponding average "Real World" fuel economy of 2008 model year vehicles per the US Environmental Protection Agency (EPA) [14]. The nodal distribution of the fuel sales is assumed to be equal to the distribution of 2016 county level gasoline sales aggregated to the nodal level [15]. This mileage is then converted into daily temperature-dependent EV charging profiles using NREL's EVI-Pro model API [16] assuming 1/3 100-mile range EVs and 2/3 250-mile range EVs (based on a fixed ratio of the NREL model); weekends and weekdays are treated identically, using a 5:2 weighted average of weekday and weekend profiles for each day[i]. This approach results in a computed average statewide EV demand of 6769 MWh/h. Because of the many assumptions involved and the closeness of this value to the net additional potential demand from heating electrification, the EV demand series is scaled to an equivalent 6716 MWh/h average demand to facilitate more direct comparison between the two. Regional and statewide computed average and peak electrified vehicle values are also shown in Supplementary Table S1.

[i] The NREL tool requires selections among fixed options for various inputs, the following of which were selected: 80% sedans, 20% SUVs; middle option of 80% for home charging preference; middle option of 75% for home charging access; equal usage of Level 1 and Level 2 home charging; 80% of work charging using Level 2 chargers; and minimum delay in charging at both home and work locations.

Supplementary Table S1: Existing and potential new nodal electricity demands.

Node	Existing Electricity Demand [MWh/h][a]		Computed Potential Net New Heating Electricity Demand [MWh/h][b]		Computed Potential New Electric Vehicle Demand [MWh/h][b]	
	Average	Peak	Average	Peak	Average	Peak
1	6383	10,467	2178	20,982	2458	5471
2	2495	4795	1059	11,347	1182	2641
3	7211	13,623	2376	13,303	1667	3642
4	2567	5933	1103	6601	1409	3081
Statewide	18,655	33,876	6716	51,088	6716	14,836

[a] NYISO [6].
[b] See the text of this section.

Internodal transmission

In SECTR-NY, both existing internodal transmission limits and costs are characterized. Existing transmission limits assumptions shown in Supplementary Table S2 are those assumed by NYISO for the year 2021 in recent system reliability simulations [17].

Supplementary Table S2: SECTR internodal existing transmission limits and costs of existing and new transmission.

Interface	Miles[a]	Existing Limits [MW][b]		New Transmission		
		West to East	East to West	Cost of New Transmission Capacity [$/MW-mi][c]		New Transmission O&M costs [$/MW-yr][d]
				$/MW-mi	$/GW	
1: Node 1 to 2	300	5000	3400	2400	720	2806
2: Node 2 to 3	150	7000	7000	4800	720	2357
3: Node 3 to 4	60	1613	220	12,000	720	277

[a] Distance between nodes taken as the distance between the representative cities of Buffalo, Albany, New York City, and Brentwood, per Google Maps.
[b] NYISO [17].
[c] See the text of this section.
[d] NREL [18].

Projecting costs of specific large-scale transmission upgrades is difficult. To evaluate the effect of transmission prices on future energy scenarios, public information on the costs of recent and proposed transmission projects in NYS was reviewed, as well as cost assumptions used in other studies of the region. References used in this assessment include: For Interface 1 (Node 1 to 2), Supplementary Table S2 shows the approximate average of $1400/MW-mi for simulated aboveground High Voltage Direct Current (HVDC) [19]; and $3614/MW-mi for underground HVDC in a NYISO study of the region [20]. For Interface 2 (Node 2 to 3), the Supplementary Table

S2 value is approximately ¾ of the cost of $6567/MW-mi for a recent NYS underground HVDC transmission installation [21] (adjusted downward due unique challenges surrounding this project). For Interface 3 (Node 3 to 4), a transmission upgrade cost of $12,000/MW-mi is assumed based on a previous underground HVDC transmission project between New Jersey and Long Island [22]. With the above per-(MW-mi) costs of upgraded transmission and the assumed distances between each node's representative city, per-GW costs of new transmission are equal at every interface.

The NREL Jobs and Economic Development Impact (JEDI) Transmission Line Model [18] is used to compute internodal O&M costs for new transmission; new transmission capacity between Nodes 1 and 2 assumes O&M costs for 500 kVAC lines, capacity between Nodes 2 and 3 assumes O&M costs for 345 kVAC lines, and capacity between Nodes 3 and 4 assumes O&M costs for HVDC reinforcements.

The annual cost of maintaining existing transmission capacity is assumed to be the total costs recovered through electricity sales based on EIA data [23]: Based on the 2019 transmission contribution to electricity unit costs ($16.9/MWh at Nodes 1 and 2; $27.3/MWh at Nodes 3 and 4) and 2019 total electricity sales (69.683 TWh at Nodes 1 and 2; 75.52 TWh at Nodes 3 and 4), total annual cost for existing transmission was computed to be approximately $3.239B.

Characterization of fossil fuel-based electricity generation

SECTR uses a simplified characterization of the existing NYS fossil fuel electricity generation fleet and new generation capacity at each node without modeling individual generators; relevant assumed values described in this section are summarized in Supplementary Table S3. As natural gas provides 96% of fossil fuel-based electricity generation in NYS [24] and generators that burn natural gas (alone or as part of dual fuel capabilities) produce 99% of NYS fossil fuel-based electricity generation [25], only existing gas-fueled electricity generation capacity (including dual fuel generators) are considered, equal to the nameplate capacity operational at the end of 2019 per NYISO [26]. The assumed cost of existing electricity generation capacity – all existing generation modeled, including natural gas, hydropower, biofuel and nuclear – at each node is derived from capacity market costs used in a recent New York State Energy Research and Development Authority (NYSERDA) study[ii]. Generator start-up costs are assumed to be $79/MW-h, the value for combined cycle gas turbines (CCGT) in a recent NREL study [3]. An electricity generation efficiency of 42.8% is assumed for existing natural gas generation based on NYS electric power sector total natural gas consumption [27] and natural gas-based electricity

[ii] The reference study [30] contains capacity market costs for New York City (NYC), Long Island (LI), Lower Hudson Valley (LHV) and Rest of State (ROS). Here, Node 1 is assumed to be 100% ROS; Node 2 to be 50% LHV and 50% ROS per the approximate actual capacity distribution [26]; Node 3 to be 87% NYC and 13% LHV per the reference study; and Node 4 to be 100% LI.

generation [28] for 2019. Modeled natural gas prices for electricity generation at each node are derived from regional natural gas avoided costs in a recent NYSERDA study[iii].

New gas-fueled generation costs are adopted based on industrial frame gas turbines (GTs) per EIA's 2020 Annual Energy Outlook [2]. These GTs have node-specific capital costs, statewide fixed and variable operations and maintenance costs, and constant 34.4% efficiency. New generator start-up costs are assumed to be $69/MW-h, the value for GTs in a recent NREL study [3]. Natural gas prices for new generators are assumed to be the same as those for existing generators at each node. Existing and new natural gas-based electricity generation capacity are constrained to be a minimum 1.189 times larger than peak generation, based on NYISO's 18.9% statewide capacity reserve margin for the 2020-2021 capability year [29].

Supplementary Table S3: Nodal gas-fueled electricity generation assumptions.

Node	Wholesale Nat. Gas Prices [$/MMBTU][a]	Existing Gas-Fueled Generation			New Gas-Fueled Generation			
		Capacity [MW][b]	Capital Cost [$/kW-yr][a]	Start-up Costs [$/MW-h][c]	Capital Cost [$/kW][d]	Fixed O&M Cost [$/kW-yr][d]	Variable O&M Cost [$/MWh][d]	Start-up Costs [$/MW-h][c]
1	2.89	3934.2	27.640	79	772	6.97	4.48	69
2	4.04	8622.5	53.440	79	772	6.97	4.48	69
3	3.67	10,249.9	101.303	79	1034	6.97	4.48	69
4	3.62	4192.7	104.600	79	1034	6.97	4.48	69

[a] NYSERDA [30].
[b] NYISO [26].
[c] Bloom et al. [3].
[d] EIA [2].

Wind power capacity and generation

Existing onshore wind capacities at each node are those active by the end of 2019 [26] as shown in Supplementary Table S4.

Wind power potential capacity and power output are based on model data developed by NREL for 126,000 potential wind sites [31,32]. First, onshore wind power potential time series data were adjusted to account for consistent over-predictions based on historical output of existing sites in NYS [33]. After this adjustment, a single wind potential timeseries was produced for each of the two upstate nodes[iv] by computing the capacity-weighted potential timeseries of all NREL-modeled sites in each node.

[iii] The reference study [30] contains natural gas avoided costs for Upstate/Western NY (UWNY), Hudson Valley (HV), and New York City and Long Island (NYC-LI). Node 1 is 100% UWNY, Node 2 is 100% HV and Node 4 is 100% NYC-LI. Node 3 is assumed to be 87% NYC-LI and 13% HV per the reference study.
[iv] Onshore wind capacity is ignored for downstate nodes 3 and 4 due to space constraints and the likelihood of a large buildout of offshore wind capacity connected to these nodes.

To determine the offshore wind potential timeseries, potential timeseries for all NREL modeled wind sites within NYS maritime boundaries are collected; these timeseries are then weighted by modeled site capacity to return a single potential timeseries. This single timeseries is adjusted based on a previously published logit transform method [33] so that the new capacity factor equals the estimate from a more recent NREL wind energy resource assessment [34], after subtracting electrical and wake losses[v]. This adjusted timeseries is applied to both downstate nodes.

High and low costs are computed for onshore (only available in upstate Nodes 1 and 2) and offshore (only available in downstate Nodes 3 and 4) wind capacity. Based on the average of costs from three recent NREL wind technology reports [35–37] and predicted cost reductions [38], a high cost of $1992/kW and a low cost of $1698/kW are assumed for onshore wind capacity. For onshore wind, fixed O&M costs of $18.10/kW-yr are applied per the 2018 Bloomberg New Energy Finance Wind Operations and Maintenance Pricing Index [39]; installations are limited to the maximum capacities given in the NREL data set [31]. Based on a review of the costs of wind energy [40], along with cost reduction estimates [38], the high cost of offshore wind capacity is set to $3583/kW; a cost curve fit to a NREL estimates of offshore wind LCOE in 2030 [41] (5% interest, 20 year lifetime) yields a low cost estimate of $2256/kW. A fixed operations and management cost of $38/kW-yr is applied for offshore wind [42], and total offshore wind installations are capped to 57.9 GW based on potential capacity in water depths less than 60m as identified by NREL [34] (See Supplementary Table S4).

Utility-scale solar capacity and generation

Existing utility-scale solar capacities at each node are those active by the end of 2019 [26] as shown in Supplementary Table S4.

The utility-scale solar potential generation time series for each node is determined by (1) identifying the capacity and location of all NYS potential grid-scale solar PV sites in a NREL model solar data set [43]; (2) computing hourly solar PV potential output using NREL's System Advisory Model [44], assuming single-axis tracking, tilted at latitude; (3) adjusting the system efficiency according to protocols specified by the California Energy Commission [45]; and (4) aggregating the individual site time series at each node, weighted by each site's capacity per the NREL data set.

High costs of new utility-scale solar PV capacity of $1341/kW at Nodes 1 and 2, and $1593/MW at Nodes 3 and 4 are adopted based on location-specific capital cost inputs to EIA's Annual Energy Outlook [2]. Low cost estimates are computed by applying a 25% cost reduction to high cost estimates, which is approximately the average of the cost reductions seen for onshore (15%) and offshore (37%) wind capacity, described above: $1006/kW in Nodes 1 and 2 and $1195/kW in

[v] From the offshore wind resource assessment [34], the potential capacity (Appendix B) and resource energy with losses (Appendix D) in water depth less than 60m areas are collected, keeping electrical losses and wake losses but removing 6% fixed losses (Appendix J). This results in a NYS offshore wind average capacity factor of 45.9%.

Nodes 3 and 4. A statewide $10.4/kW-yr fixed O&M cost is set for new solar capacity based on a recent NREL benchmark for utility-scale tracking PV [46]. To account for space limitations, the maximum potential utility-scale solar PV capacity is determined by county and then aggregated to the nodal level, per Supplementary Table S4. For each county, the maximum capacity is based on 1) the smaller quantity of (a) existing cropland, per the 2017 USDA Census of Agriculture [47], or (b) 10% of the county's total land area; and 2) an assumed 8.5 MW/acre [48].

Supplementary Table S4: Nodal existing and maximum wind power and utility-scale solar capacities.

	Existing Capacity [MW]		Maximum Potential Capacity [MW]		
Node	Onshore Wind[a]	Utility-scale Solar[a]	Onshore Wind[b]	Offshore Wind[c]	Utility-scale Solar[d]
1	1985.25	0	32,402	0	212,710
2	0	0	4376	0	44,899
3	0	0	0	57,938	481
4	0	56.5	0		2743

[a] NYISO [26].
[b] Draxl et al. [31].
[c] Musial et al. [34].
[d] See the text of this section.

Behind-the-meter solar capacity and generation

Nodal BTM solar capacity is imposed exogenously on the optimization based on a user-provided year and a nodal capacity distribution, itself determined by a NYISO-projected 9 GW solar capacity scenario [49]. Statewide BTM solar capacity is based on a logistic growth function of the general form shown in Supplementary Eq. (S40) fit to historical capacity data for the years 2000-2019 [50]:

$$\sum_{i \in I} X_{btm-solar,i} = \frac{K}{1 + Qe^{-B(year-M)*1/v}} \quad \text{(S40)}$$

where K = 10,982.023; Q = 1.680925e-4; B = 0.1202713, M = 1995.067; v = 4.955324e-6.

Existing nodal capacity as of the end of 2019 [50] and projected distribution computed per Supplementary Eq. S40 for example years are shown in Supplementary Table S5.

Supplementary Table S5: Nodal behind-the-meter (BTM) solar capacity

	BTM Solar capacity (MW) for given year			
Node	Current[a]	2030	2040	2050
1	562	2109	3009	3348
2	523	2364	3372	3752
3	293	1096	1564	1740
4	259	1039	1482	1649

[a] At the end of 2019 per NYSERDA [50].

The BTM PV generation time series for each node is determined by (1) selecting a representative city for each NYISO zone from those in the NREL National Solar Radiation Database [51]; (2) computing hourly solar PV potential output using NREL's System Advisory Model [44], assuming a fixed axis, tilted at latitude; (3) adjusting the system efficiency according to protocols specified by the California Energy Commission [45]; and (4) aggregating zonal time series at each node weighted by zonal capacities in the NYISO-projected 9 GW solar capacity scenario [49].

Energy storage

Existing battery storage power capacity was extracted from the EIA energy mapping system [52], and existing battery storage energy capacity was determined from news reports and websites corresponding to recently installed projects[vi]; these quantities are presented in Supplementary Table S6. Although the SECTR General Formulation allows per-unit power capacity and per-unit energy capacity cost components, for the present analyses only energy capacity costs are included. High and low costs are set based on the "Mid" and "Low" cost projections for 2030 from NREL [53]: $208/kWh and $144/kWh, respectively. A power-to-energy ratio of 0.25 kW/kWh is assumed based on common 4-hour battery systems, with 94.6% charge and discharge efficiencies based on the 89.5% roundtrip efficiency of a commercially available battery storage system [54]. A 10-year lifetime [55] is adopted for modeled batteries. Batteries are also assigned a self-discharge rate of 0.1%/hr.

Supplementary Table S6: Existing nodal battery energy and power capacity.

	Existing Battery Capacity	
Node	Battery Energy [MWh]	Battery Power [MW]
1	5.2[a]	3[a]
2	80	20[b]
3	0	0
4	65[c]	10[c]

[a] Battery capacities taken from [56,57].

[b] Key Capture Energy [58]; the facility is assumed to be a 4 hour battery system.

[c] Battery capacities taken from [59,60].

[vi] Node 1: East Pulaski BESS [56] and Lockheed Martin RMS [57]. Node 2: KCE NY 1 assumed to be 4 hour battery system [58]. Node 4: East Hampton Energy Storage Center [59] and Montauk Energy Storage Center [60].

For long-term storage, the use of hydrogen electrolysis and combustion in a gas turbine is assumed, with model-selected deployment analogous to battery storage based on cost components for both power capacity and energy capacity. A power capacity cost of $3013/kW is adopted based on a recent study [61] for Nodes 1 and 2; the same capital cost adjustment for GTs is then applied for Nodes 3 and 4, resulting in $4036/kW. For hydrogen storage capital costs, a per-unit energy cost of $0.35/kWh is set for geologic storage in Node 1 based on an NREL study (and adjusting from 2008 dollars to 2020 dollars) [62]. For other nodes, hydrogen storage is assumed to occur in carbon fiber storage tanks given the lack of geologic formations for storage and higher population density; a storage cost of $8.29/kWh is applied based on annually updated Department of Energy hydrogen storage cost analysis [63]. A fixed operations cost of $48.87/kW-yr is assumed based on an earlier study [64]. Charge and discharge efficiencies of 59.2% are adopted based on 35% roundtrip efficiency in a recent NREL analysis [65] referencing an earlier study [66]. A self-discharge rate of 0.1%/hr is set.

Nuclear power

The nuclear power landscape in NYS is evolving, as the last operational generator of the Indian Point two-generator plant in Node 3 shuttered on April 30, 2021 [67], and nuclear generators in Node 1 have been subsidized in recent years. To investigate the impact of capacity retirements, the SECTR-NY formulation can either include or ignore these nuclear generators. Nuclear capacity is distributed across all four model nodes per NYISO [26] as shown in Supplementary Table S7 (which for clarity shows no nuclear at Nodes 2 and 4). Electricity generation is assumed to be constant throughout the simulation period and equal to the average electricity production of those generators in 2019 according to NYISO [26]. The price of nuclear electricity at each node is computed from the average 2019 day-ahead locational based marginal pricing (LBMP) [6] of each nuclear generator at each node, weighted by the 2019 total net electricity generation [26] of each of those generators. The price at Node 1 is increased to account for subsidies of the nuclear generators at that node, funded by Zero Emission Credits (ZECs). Per Supplementary Eq. (S41), the per energy unit subsidy is computed from the 2020 compliance year ZEC rate [68], NYISO's 2020 baseline demand forecast [26], and the constant output of nuclear electricity at Node 1 from Supplementary Table S7.

$$\left\{\begin{matrix}Nuclear\ Price\ Subsidy \\ at\ Node\ 1\end{matrix}\right\} = \frac{\left\{\begin{matrix}2020\ Compliance \\ Year\ ZEC\ Rate\end{matrix}\right\} \times \left\{\begin{matrix}NYISO\ 2020\ Baseline \\ Demand\ Forecast\end{matrix}\right\}}{\{Constant\ Electricity\ Generation\ at\ Node\ 1\}} \quad \text{(S41)}$$

The assumed cost of existing nuclear electricity generation capacity at each node is the same as described above under "Characterization of fossil fuel-based electricity generation."

Supplementary Table S7: Nodal existing nuclear power characteristics

Node	Generation Capacity [MW][a]	Constant Electricity Generation [MWh/h][a]	Capacity Cost [$/kW-yr][b]	Electricity Price [$/MWh][c]
1	3536.8	3207	27.640	37.94
2	0	0	N/A	N/A
3	2311	1906	101.303	26.82
4	0	0	N/A	N/A

[a] NYISO [26].
[b] NYSERDA [30].
[c] See the text of this section.

Hydropower

The methodology for creating hydropower fixed and flexible generation time series is described in a recent paper [4]. Actual monthly hydropower output by facility is collected for 2007-2012[vii] from EIA Form 923 [69], and then is aggregated at each node. The two largest NYS hydropower facilities (both located at Node 1) operate near their maximum capacity given available stream flows; accordingly, fixed hourly time series are provided for these generators. The remaining hydropower generation and capacity in Nodes 1 and 2 are considered to be flexible with provided daily total electric energy generation requirements. Total fixed and flexible hydropower capacities are computed from the nameplate capacities operational at the end of 2019 [26]. Hourly generation is determined endogenously by the hydropower methodology detailed in the General Formulation. Hydropower-generated electricity prices are based on recent prices for such electricity in NYISO's day-ahead market[viii]. The assumed cost of existing hydropower electricity generation capacity at each node is the same as described above under "Characterization of fossil fuel-based electricity generation." The values described here are summarized in Supplementary Table S8.

[vii] Monthly generation quantities for 2007-2012 are used to align with the wind, solar, and demand time series.
[viii] All based on 2019 hourly day-ahead LBMP [6] and weightings by total 2019 electricity production [26]: Node 1 cost is the weighted average LBMP for Moses Niagara and St. Lawrence hydropower facilities; Node 2 is the weighted average LBMP of the four highest producing hydropower facilities at that node (62% of total hydroelectricity production at that node).

Supplementary Table S8: Existing hydropower characteristics

	Average Generation [MWh/h][a]		Capacity [MW][b]		Capacity Cost [$/kW-yr][c]	Electricity Price [$/MWh][d]
Node	Fixed	Flexible	Fixed	Flexible		
1	2395	328	3948	769.4	27.640	18.47
2	0	270	0	608.7	53.440	28.02
3	0	0	0	0	N/A	N/A
4	0	0	0	0	N/A	N/A

[a] EIA [69].
[b] NYISO [26].
[c] NYSERDA [30].
[d] See footnote *vii*.

Biofuel-based electricity generation

SECTR-NY classifies various electricity generation feedstocks as "biofuels": wood and wood waste, biogas, and solid waste. In NYS, biofuel capacity is distributed across all four model nodes per NYISO [26] as shown in Supplementary Table S9. Intraday biofuel electricity generation is flexible as described in the Main Text; maximum daily electricity generation is assumed to be constant throughout the simulation period and equal to the average daily electricity production of those generators in 2019 according to NYISO [26]. Biofuel-generated electricity prices are based on recent prices for such electricity in NYISO's day-ahead market[ix]. The assumed cost of existing biofuel-based electricity generation capacity at each node is the same as described above under "Characterization of fossil fuel-based electricity generation."

Supplementary Table S9: Nodal existing biofuel characteristics

Node	Generation Capacity [MW][a]	Daily Electricity Generation [MWh][a]	Capacity Cost [$/kW-yr][b]	Electricity Price [$/MWh][c]
1	258.0	3289.041	27.640	20.66
2	45.0	473.425	53.440	27.41
3	59.7	1046.575	101.303	27.05
4	142.2	2445.479	104.600	32.29

[a] NYISO [26].
[b] NYSERDA [30].
[c] See footnote *ix*.

[ix] All based on 2019 hourly day-ahead LBMP [6] and weightings by total 2019 electricity production [26]: Node 1 cost is the average LBMP for the four highest producing biofuel facilities at that node (58% of total biofuel electricity production at that node); Node 2 is the average of Zone F and G LBMP; Node 3 is the average LBMP for the 1 biofuel facility at that node; Node 4 is the weighted average LBMP of all four biofuel facilities at that node.

External imports

NYISO currently imports significant quantities of low-carbon electricity from Hydro-Quebec (HQ), a net average of 1247 MWh/h in 2019 [26]; as such, electricity imported at this interface with Node 1 is included as a decision variable constrained to the maximum interface limit specified by NYISO (1.5 GW) [6]. A cost of $22.13/MWh is attributed to this imported electricity based on average 2019 day-ahead LBMP [70] and including capacity market payments for 1114 MW capacity per NYISO [71].

NYS regulators are nearing approval for plans for the Champlain Hudson Power Express, a 1250 MW HVDC transmission line that would bring hydropower-produced electricity from Quebec to New York City [21], which is also included in recent NYC local legislation [72]. As such, additional electricity import into Node 3 is included in future energy system scenarios. The precise cost of this electricity supply is unknown; however, a price of $70/MWh is adopted based on publicly available information, personal and public conversations about the project, and various possible financing parameters[x]. The line is assumed to provide 1125 MWh/h continuous based on the approximate 90% capacity factor of existing upstate Hydro-Quebec import lines [6] and an understanding of the project from public and personal conversations.

Imports from other external control areas are ignored to avoid characterizing or modeling future developments in regions that currently rely largely on fossil fuel-based electricity generation.

Greenhouse gas emissions

As accounted by NYSERDA, NYS energy sector emissions constitute 84% of total statewide GHG emissions (measured in equivalent global warming potential of carbon dioxide, CO_2e) as of 2016 [73]. The remaining 16% of GHG emissions comes from industrial processes, agriculture, and waste.

In New York's Climate Leadership and Community Protection Act (CLCPA), statewide GHG emissions accounting includes GHGs produced in NYS and GHGs produced outside NYS that are associated with imported electricity and fossil fuels [74]. Supplementary Table S10 shows emissions factors for carbon dioxide (CO_2), methane (CH_4), and nitrous oxide (N_2O) compiled from a variety of sources; the table also includes values for carbon dioxide equivalent (CO_2e). CO_2e is a single metric that combines the effect of multiple GHGs based on their global warming potential (GWP). CLCPA requires GWP values based on the amount of warming impact relative to CO_2 when integrated over a 20-year time frame. Here, respective GWPs of 86 for CH_4 and 264 for N_2O are used, in accordance with the Intergovernmental Panel on Climate Change (IPCC) Fifth Assessment Report (AR5) [75]. CH_4 emissions, particularly for natural gas, are largely dependent on venting

[x] Our calculations are generally in the $65-70/MWh range based on the project website's lower bound capital cost [21], higher potential upfront costs that have been discussed publicly, various annualization periods, average HQ export revenues ($1441M on 33.7 TWh in 2019 [85]), and the approximate 90% capacity factor of existing upstate Hydro-Quebec import lines [6].

at wellheads and leakage in transmission and distribution infrastructure; understanding these effects is the subject of ongoing research, but recent efforts focused on New York State provide a reliable reference point [76].

Supplementary Table S10: Emissions factors [g/MJ] for GHG contributors

Energy source	CO_2	CH_4	N_2O[f]	CO_2e
Coal	92[a]	0.185[c]	$1.52 \cdot 10^{-3}$	108.31
Petroleum	73[b]	0.093[d]	$5.69 \cdot 10^{-4}$	81.15
Natural Gas	55[a]	0.641[e]	$9.48 \cdot 10^{-5}$	110.18

[a] Based on high-heating values per Hayhoe et al. [77] as documented by Howarth et al. [76].
[b] CO_2 emission factor for petroleum is the high-heating value from Howarth et al. [78] as reported by Howarth et al. [76].
[c] As computed by Howarth et al. [76] based on the ratio of total methane emissions during coal mining and total coal production in the U.S. in 1990 from IPCC reporting [79], with a coal heating value of 27 MJ/kg [78].
[d] Based on CH_4 emissions from petroleum production from the National Energy Technology Laboratory (NETL) [80] as documented by Howarth et al. [76].
[e] Computed from assumptions of: CH_4 emission rate of 3.6% as used for NYS in Howarth et al. [76] based on a range computed by Alvarez et al. [81] and Howarth et al. [78]; natural gas to be 93% CH_4 [82]; and a high-heating value of 52.2 MJ/kg for natural gas in the U.S. market [83].
[f] EPA [84].

Per the targets set in the CLCPA [74], emissions reductions relative to a 1990 reference value are computed. Reference CO_2 and CH_4 emissions for electricity, buildings, industrial, transportation are calculated by using the 1990 EIA fuel consumption estimates [12] and emission factors in Supplementary Table S10; CO_2 and CH_4 emissions for electricity imports in 1990 are taken directly from Howarth et al. [76]; CO_2 and CH_4 emissions for waste incineration and all N_2O emissions in 1990 are from the NYSERDA inventory of GHG in NYS [73]. Thus an $\varepsilon_{baseline}$ of 302.770 $MMtCO_2e$/year is computed, per Supplementary Table S11. Supplementary Table S11 further delineates emissions that are fixed in the model and those that are variable: variable emissions can change as computed by the model for a given user-defined scenario and as described by Eqs. (11-15) in the Main Text.

Current NYS electricity emissions are calculated by using SECTR to model a "current scenario". The current scenario includes all existing NYS energy infrastructure parameterized and discussed above, and assumes current capacities of wind and solar power, no additional electrification of vehicle or heating demand, and no generation from the Indian Point nuclear facility. Using the natural gas emissions factors in Supplementary Table S10 and the model-returned amount of natural gas generation needed to meet the existing electricity demand, current electricity emissions of 84.889 $MMtCO_2e$/year are computed, per Supplementary Table S11. Since SECTR-NY assumes the modeled electricity sector can be fully decarbonized, these emissions are considered variable.

Total fossil fuel usage for heating, $F_{heat,tot,i}$, is computed from the heating model [7] described above; portions of this fossil fuel usage are attributed to natural gas, fuel oil, and propane based on the 2018 residential and commercial usage of these fuels [12]. Annual heating GHG emissions,

ε_{heat}, are calculated as 110.853 $MMtCO_2e$/year averaged over the six-year computation period based on the emissions factors for natural gas and petroleum (for fuel oil and propane) in Supplementary Table S10. As SECTR-NY assumes that NYS heating demand can be fully electrified, these emissions are considered variable in Supplementary Table S11.

Transportation sector emissions are determined from the 2018 EIA fuel consumption estimates [12] that are used to calculate statewide vehicle energy demand as described above. Gasoline and diesel consumption for transportation that can be electrified, $F_{veh,tot}$, and the petroleum emissions factor in Supplementary Table S10 are used to compute 73.703 $MMtCO_2e$/year variable emissions for vehicles included in the model electrification scope, ε_{veh}. Aviation fuel, hydrocarbon gas liquids, jet fuel, lubricants, residual oil, and natural gas consumption for transportation listed in the same EIA dataset [12] are considered fixed and constitute transportation emissions outside the scope of the model, $\varepsilon_{transp,other}$. From this usage data and the appropriate emissions factors from Supplementary Table S10, $\varepsilon_{transp,other}$ is computed to be 21.956 $MMtCO_2e$/year, a quantity fixed in every model run.

Industrial emissions, ε_{ind}, are calculated from the 2018 EIA fuel consumption estimates [12] and the appropriate emissions factors from Supplementary Table S10. Here, coal, natural gas, and petroleum products result in computed total emissions of 19.365 $MMtCO_2e$/year; this quantity is fixed in every model run.

Supplementary Table S11 also displays emissions from waste incineration in New York for the current system. In SECTR-NY model scenarios, waste incineration is excluded per the CLCPA [74]; as this emissions quantity is set to 0 in all model runs, it is presented as variable.

Supplementary Table S11: Relevant aggregate greenhouse gas emissions ($MMtCO_2e$/year)

Emissions Source	1990 Reference Emissions	Current Emissions as Modeled	
		Variable	Fixed
Electricity	86.772	84.889[a]	0
Electricity Imports	1.909	0	0[b]
Heating (Buildings)	100.468	110.853	0
Industrial	32.824	0	19.365
Transportation	79.532	73.703	21.956
Waste Incineration	1.265	2.784[c]	0
Total	302.770	272.229	41.321
		313.550	

[a] Based on SECTR-NY model of current system as described in this section.

[b] Electricity imports are only considered from hydropower generation.

[c] This quantity represents the 2016 value from NYSERDA inventory for waste incineration [73]. In SECTR model runs, it is set to zero.

Seasonal distribution of demand and renewable generation potentials

Existing electricity demand, electrified demand, and the renewable generation potentials of wind and solar resources used in SECTR-NY simulations all demonstrate substantial seasonal variability. Fig. 2 in the main text contains monthly values for the mean and maximum existing electricity demand; the means and maximums of existing electricity demand combined with either electrified heating or transport; and the means of onshore wind, offshore wind, and utility-scale solar generation potentials. From the top and middle panels in Fig. 2, one observes that electrified heating increases average and peak electricity demands in the winter months: Full electrification of heating increases average load by up to 15 GWh/h and peak load by up to 52 GWh/h. In contrast, electrification of transport has smoother effect. With 100% transport electrification, average load rises by 6 to 8 GWh/h in all months of the year, with the larger increases coming during the winter due to the inverse relationship between temperature and EV charging demand. The effect on peak load is similarly consistent: Peak electricity demand increases by 12 to 15 GWh/h in all months.

Wind and solar generation potentials in NYS also display a strong seasonal dependence. Offshore and onshore wind potentials both peak in the winter months, reaching an average of 0.57 $MWh_{generation}/MW_{installed}$ and 0.40 $MWh_{generation}/MW_{installed}$, respectively; in the summer months, average generation for each decreases by approximately 50%. In contrast, utility-scale solar capacity offers peak generation potentials during the summer months, up to an average 0.26 $MWh_{generation}/MW_{installed,}$, while winter months see this quantity drop to 0.10 $MWh_{generation}/MW_{installed}$.

Taking all three panels of Fig. 2 together, a clear seasonal alignment is identified between electrified heating demand and wind generation potential, indicating that electrified heating may prove effective in integrating large amounts of installed wind capacity. Moreover, summer-peaking solar generation is well-suited to meet summer loads in NYS, both those that currently exist and those that are increased by transport electrification.

S3 Supplementary Results

Supplementary Section S3 contains additional results for the SECTR Baseline configuration; results that investigate the impact of SECTR system parameterization assumptions; and main text results for different heating and vehicle electrification rates (HVEs) and low carbon electricity percents (LCPs).

S3.1 Additional Baseline configuration results

Supplementary Figure S2 presents an analogous plot to Fig. 3(a), but with a continuous 3.2 GWh/h of upstate nuclear generation present. Here, nuclear generation allows for approximately 10% lower LCOEs on average at the simulated scenarios, cost savings that grow larger at higher LCPs. However, the addition of nuclear generation does not change the overall shape of Fig. 3(a), and accordingly the same conclusions are reached: 1) Emissions reductions can be achieved at lower LCOEs by prioritizing electrification of heating and vehicles in conjunction with deployment of solar and wind, as opposed to the latter by itself, and 2) system costs increase substantially above 70-80% LCPs.

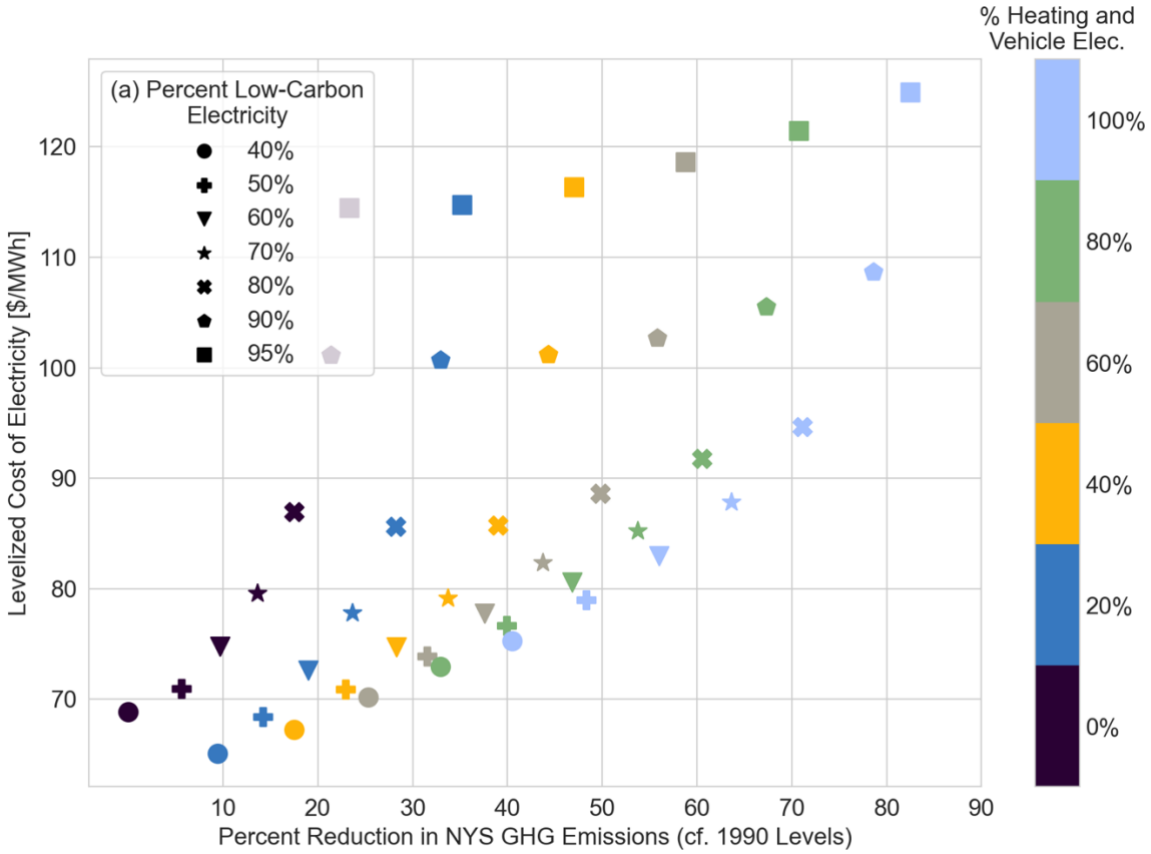

Supplementary Figure S2: LCOE vs. percent reduction in NYS GHG emissions (compared to 1990 levels). Marker shape indicates percent low-carbon electricity (LCP), and marker color indicates heating and vehicle electrification (HVE). For scenarios shown, all low-carbon electricity generation is from wind, solar, nuclear, and hydropower.

Next explored are the effects of either increased HVE or LCP on peak gas generation, average gas generation, low-carbon electricity generation, and battery storage throughput. In evaluating the peak gas generation characteristics, increasing electrification at a set LCP results in substantial winter peaks: Supplementary Figure S3(a) presents the monthly peak to annual average gas generation ratio at 60% LCP for 0%, 40% and 80% HVE. At 80% HVE, additional, peaky heating demand causes January gas generation peaks of 46.9 GWh/h, equal to 4.6 times the annual average, compared 15.9 GWh/h at 0% HVE with a peak-to-average ratio of 2.7. In contrast, the July peak only increases from 22.4 GWh/h at 0% HVE to 25.5 GW at 100% HVE. Supplementary Figure S3(b) shows that there are no equivalent seasonal effects to increasing the LCP at 40% electrification. However, increasing the LCP to 80% and 95% results in lower average gas generation (4.0 GWh/h and 1.0 GWh/h, respectively, compared to 8.0 GWh/h), quantities which result in substantial peak-to-average ratios (above 20 in December and January for the 95% LCP).

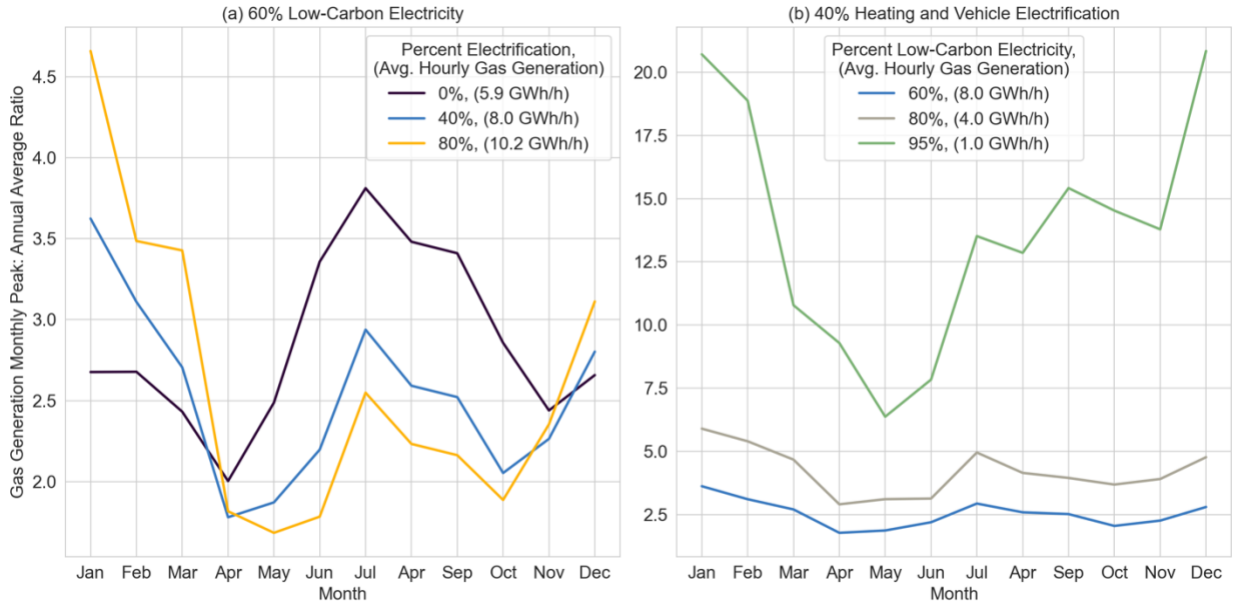

Supplementary Figure S3: Monthly peak to annual average gas generation ratios for (a) scenarios containing 60% low carbon electricity with increasing amounts of electrification; and (b) scenarios containing 40% electrification with increasing percents low-carbon electricity.

Increasing electrification at a set LCP has a similar seasonal shift on average gas generation, shown in Supplementary Figure S4(a). For the same 60% LCP and 0%, 40%, and 80% HVEs, increased electrification results in higher average winter gas generation – in absolute terms and relative to the annual average – and lower relative generation during the summer. In January, 0% HVE corresponds to an average 5.3 GWh/h of gas generation, or 0.9 times the annual average; 100% HVE increases this to 16.3 GWh/h, or 1.6 times the annual average. Again, this increase in average generation is attributable to the higher amounts of peaky heating demand on the system: Heating demand proves difficult to meet with low-carbon electricity and is accordingly satisfied by dispatchable gas generation. The suitability of gas generation in meeting electrified heating demand also explains the relative decreases in gas generation during summer months.

As the same LCP needs to be achieved despite increased winter gas generation, gas generation during the summer is reduced (1.2 times the annual average with 80% HVE compared to 1.8 times at 0% HVE in the month of July), as this less-peaky demand can more easily be met by a combination of solar generation and battery storage.

Supplementary Figure S4(b) demonstrates that raising the LCP from 60% to 95% increases the January gas generation from 1.3 to 2.5 times the annual average, a shift that indicates the costliness of meeting electrified heating demand with only low-carbon generation and battery storage. In contrast, gas generation in the shoulder seasons is the first to be displaced by low-carbon generation, due to 1) the high productivity of onshore wind, offshore wind, and solar resources, and 2) the lack of peaky heating demand during these months.

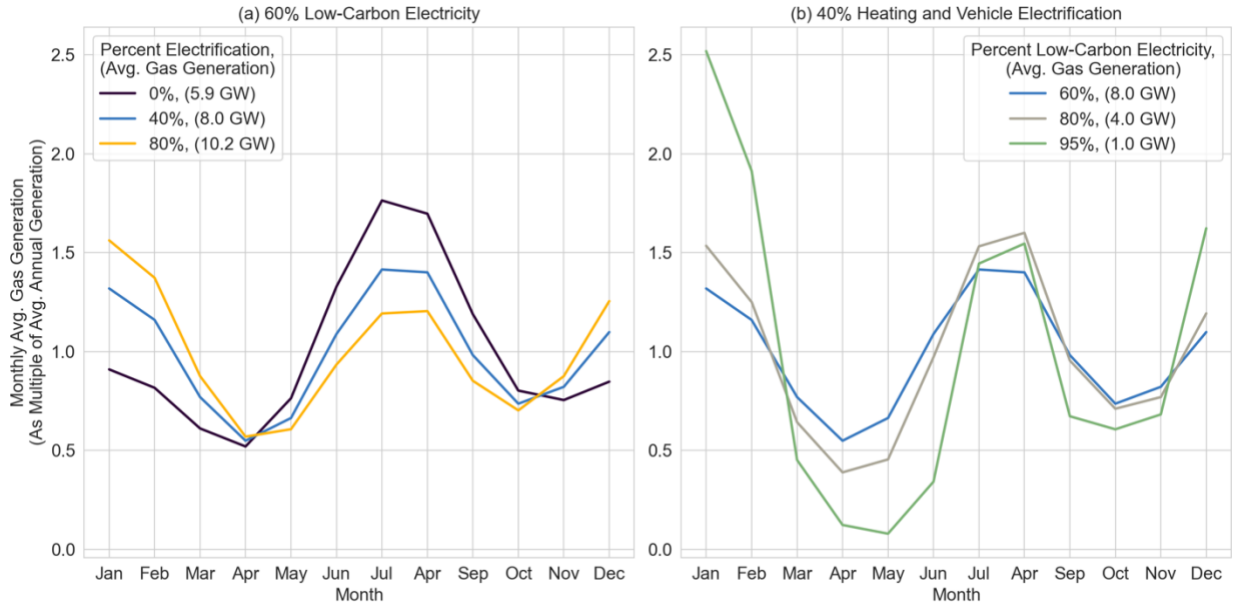

Supplementary Figure S4: Monthly gas generation as a multiple of the annual average for scenarios containing (a) 60% low-carbon electricity with increasing amounts of electrification; and (b) 40% electrification with increasing percents low-carbon electricity.

Evaluation of monthly battery storage behavior reinforces the findings presented in main text. Increasing electrification at 60% low-carbon electricity shifts battery throughput towards summer months when battery storage is well-paired with the daily cycles of productive solar generation, per Supplementary Figure S5(a). While this relative seasonal shift is apparent in the changing shapes of the normalized throughput curves, the absolute seasonal difference in battery throughput is not as stark: Increasing HVE from 0% to 80% only raises battery throughput by an average 1.0 GWh/h, indicating that battery output is not utilized to meet a significant portion of demand at 60% LCP. In contrast, battery throughput increases substantially in the summer months – in both absolute and relative terms – and experiences a relative drop during the shoulder seasons as LCP increases from 60% to 95% at 40% HVE (Supplementary Figure S5(b)). At 95% LCP, battery throughput reaches an average of 3.1 GWh/h in August (1.4 times the annual average), a quantity that is double the average throughput in April (1.6 GWh/h); to

compare, the 60% LCP scenario contains average throughputs in August and April both roughly equal to the annual average of 0.6 GWh/h. From this figure, one concludes that pairing batteries with productive solar generation during summer months provides a cost-effect method of meeting additional load with low-carbon electricity. It is also notable that this effect is substantially greater when increasing the LCP at a given HVE, due to the greater amounts of excess low-carbon generation present in these scenarios.

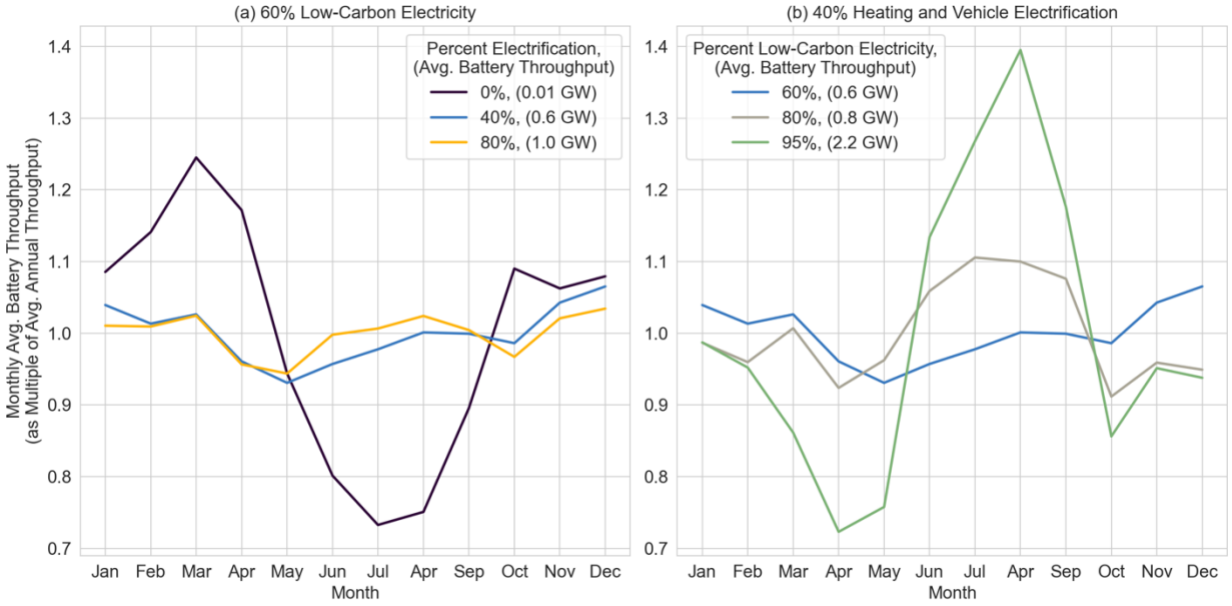

Supplementary Figure S5: Monthly battery throughput as a multiple of average annual throughput. Results are presented for scenarios containing (a) 60% low carbon electricity with increasing amounts of electrification; and (b) 40% electrification with increasing percents low-carbon electricity.

S2.2 Impact of existing system parameterization

To understand the impact of SECTR baseline parameters and how different parameterizations affect model results, two additional configurations are evaluated: A 'Greenfield' configuration and a 'Greenfield with Constant Costs' configuration. The Greenfield configuration represents a type of parameterization often seen in the capacity expansion modeling literature: This configuration includes no existing solar, wind, gas, biofuel, or transmission capacity; and no existing biofuel generation. The Greenfield with Constant Costs configuration combines the greenfield parameterization with homogenous nodal costs, which are calculated via a weighted average of the costs associated with the returned capacity and generation quantities from the Greenfield configuration model solution.

All configurations are evaluated at two scenarios, one representing a combination of a high LCP and a low HVE (referred to as the high LCP scenario), and the other representing a combination of a lower LCP and a higher HVE (referred to as the low LCP scenario). In both scenarios, the GHG reduction is set to 40%. For the high LCP scenario, electrification of heating and transport is set

to 40% and the LCP is determined by the model; for the low LCP scenario, LCP is set to 60% and the HVE is determined by the model. To ensure equivalent LCPs across configurations, the efficiency of new gas turbines in a Greenfield-based configuration is set to the weighted average efficiency of existing and new generation in the corresponding Baseline scenario.

Supplementary Table S12: Select computed characteristics of Baseline and Greenfield configurations.

	Configuration Parameters			Model-returned Generation and Storage Capacities (Cap.) and Transmission (Tx.) Characteristics							
Configuration	% GHG[a]	% HVE[b]	% LCP[b]	Total Gas Cap. [GW]	Total Upstate Battery Cap. [GW]	Total Downstate Battery Cap. [GW]	Total Pos. Tx. Cap. [GW-mi][c]	Total Rev. Tx. Cap. [GW-mi][d]	Avg. Pos. Tx. Util. %[c]	Existing Cap. LCOE [$/MWh][e]	Total LCOE [$/MWh]
Baseline	-40	40	81.7	27.2	7.3	1.2	2646.8	2287.4	24.3	27.0	96.4
Baseline	-40	64.8	60	47.2	2.8	3.9	2646.8	2083.2	28.1	23.7	83.5
Greenfield	-40	40	81.3	26.1	8.8	3.5	2473.3	0.0	31.7	0.8	86.5
Greenfield	-40	64.3	60	48.4	2.6	3.9	1371.0	0.0	41.7	0.7	75.8
Greenfield w. Constant Costs	-40	40	81.3	25.7	10.9	2.2	2339.8	0.0	27.3	0.8	86.7
Greenfield w. Constant Costs	-40	64.4	60	48.0	5.7	2.7	629.0	5.3	29.9	0.7	75.0

[a] '% GHG' refers to the percent change in greenhouse gas emissions compared to the 1990 reference values. Negative values indicate reductions.
[b] LCPs/HVEs are not identical across configurations due to slight differences in model-computed electricity imports given the specified GHG reduction and the HVE/LCP.
[c] 'Pos.' refers to "positive" upstate-to-downstate transmission directionality, i.e. from Node 1 to 2, Node 2 to 3, and Node 3 to 4.
[d] 'Rev.' refers to "reverse" downstate-to-upstate transmission directionality, i.e. from Node 4 to 3, Node 3 to 2, and Node 2 to 1.
[e] The costs of maintaining existing gas, hydropower, biofuel, and transmission capacity constitute the cost portion of 'Existing Capacity LCOE.'

Supplementary Table S12 presents a comparison of model-selected gas, battery, transmission, and LCOE characteristics. Here, both Greenfield configurations (with and without constant costs) contain LCOEs approximately 10% lower than in the fully-parameterized Baseline configuration, regardless of the combination of HVE/LCP. As the Greenfield configurations do not include any existing gas, biofuel, or transmission capacity, the fixed costs associated with maintaining this infrastructure (see 'Existing Cap. LCOE' column) drop to nearly $0/MWh, a reduction that causes the total LCOE decline. Moving from the Baseline to the Greenfield configuration, an average

60.2% decline in total installed transmission capacity is observed across both scenarios, with reverse transmission being completely eliminated; moving to the Greenfield with Constant Costs configuration causes an average 69.2% decline. Accordingly, the transmission capacity that is installed in the positive direction is utilized more frequently, a trend which is particularly pronounced in the Greenfield configuration results, due to lower amounts of installed downstate gas generation (see following Supplementary Figure S6).

For the high LCP scenarios in the two greenfield configurations, less transmission capacity and lower amounts of installed gas generation are compensated by increased battery capacity: The Greenfield configuration contains 2.8 GW additional storage capacity (a 29.4% increase), while the Greenfield with Constant Costs configuration contains 3.6 GW additional storage capacity (a 37.9% increase). This larger quantity of installed battery capacity is less prominent in the low LCP scenarios, due to their lower need for low-carbon electricity shifting; however, the low-LCP scenario in the Greenfield with Constant Cost configuration contains 1.7 GW more battery capacity than its Baseline analogue, an increase of 25.4%

Supplementary Figure S6 displays the change in gas capacity and generation characteristics across the three configurations. Here, the spatial heterogeneity of SECTR-NY results is investigated by splitting NYS into upstate and downstate regions[xi]. Upstate NYS contains the state's onshore wind capacity, low-cost utility-scale solar, and existing low-carbon generation, while downstate NYS contains substantial electricity demand in and around New York City and offshore wind capacity. These differences in regional characteristics results in distinct system behavior on either side of the interface between Nodes 2 and 3.

Comparing results across configurations, the top row – representing the high LCP scenario – contains a 7.1 GW shift in gas capacity from downstate to upstate nodes when changing from the Baseline to the Greenfield configuration, due to the relatively higher cost of downstate gas capacity. Adopting constant nodal costs causes a smaller shift: When all new capacity has the same cost, the high LCP scenario shifts 1.8 GW gas capacity towards downstate regions compared to its equivalent Baseline configuration. In the low LCP scenarios (bottom row of Supplementary Figure S6), a consistent shift from upstate to downstate gas generation capacity is observed: The Greenfield configuration contains a shift of 5.4 GW, while the Greenfield with Constant Costs configuration contains a shift of 12.0 GW.

[xi] 'Upstate' is defined as a region containing Nodes 1 and 2; 'downstate' refers to a combination of Nodes 3 and 4.

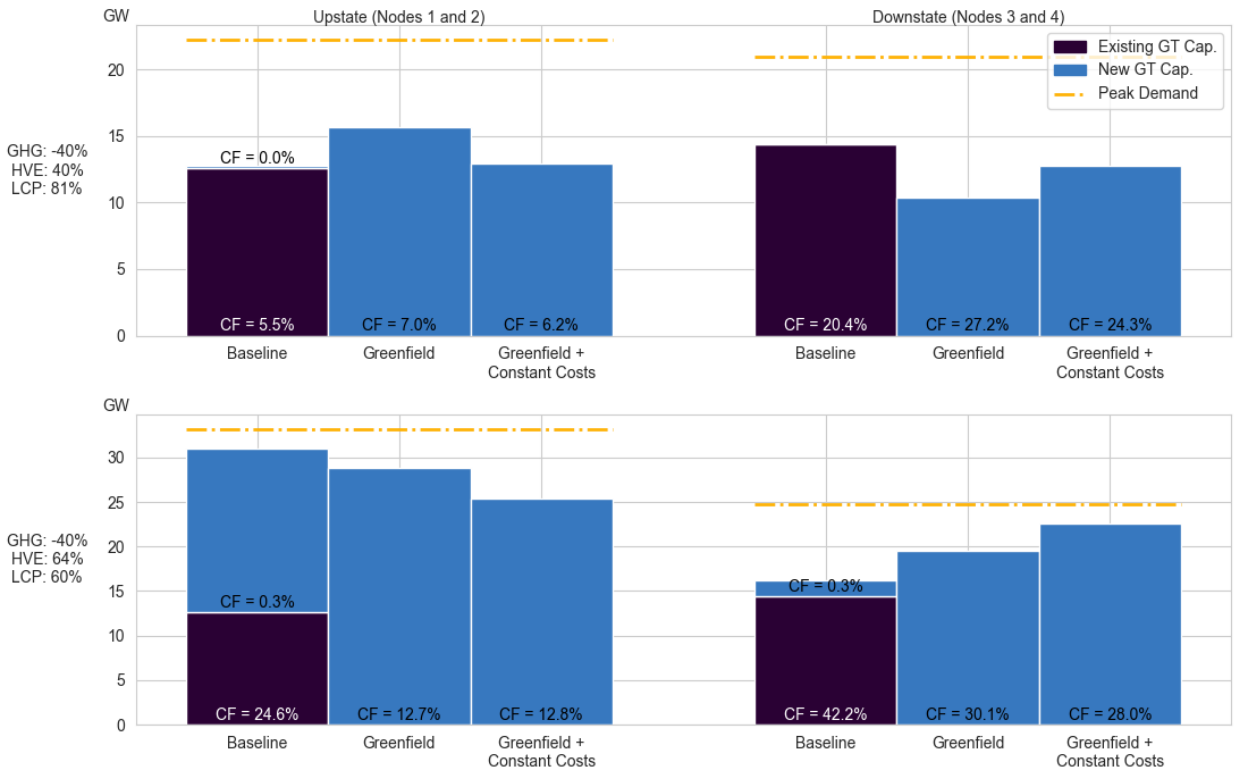

Supplementary Figure S6: Existing and new gas capacity, distribution, and capacity factors (CF), shown with peak demand, for upstate and downstate New York State regions. The top row presents results for the high low-carbon electricity percent (LCP) scenario; the bottom row presents results for the LCP scenario.

Both scenarios reveal the low capacity factors (CFs) of gas capacity in energy systems that achieve 40% GHG reduction, regardless of the configuration. In the top row, the high percent low-carbon electricity means that gas generation meets 19% of demand; this corresponds to capacity factors less than 7% upstate and less than 28% downstate. Here, CFs are lower upstate as this where the bulk of the renewable generation capacity is located. In comparison, gas generation CFs are higher on average for the low LCP scenario despite the larger amounts of GT capacity required to meet the additional electrified load: The looser low-carbon electricity constraint means that gas generation can satisfy approximately 40% of the demand. The outlier to this trend is the new gas capacity installed upstate in the Baseline configuration. For this scenario, 18.4 GW of new upstate capacity generates an average of 62.7 MWh/h, and 1.8 GW of new downstate capacity generates an average of 5.7 MWh/h, both corresponding to rounded CFs of 0.3%.

S3.3 Main text figures presented at different rates of heating and vehicle electrification and different percents low-carbon electricity

Supplementary Figures S7-S8 display versions of Fig. 5 at different HVEs and LCPs; Supplementary Figures S9-S10 display versions of Fig. 7 at different HVEs; and Supplementary Figures S11-S12 display versions of Figs. 8-9 at different HVEs. These figures demonstrate that the results presented in the main text are not unique to the selected percents low-carbon electricity or electrification rates therein.

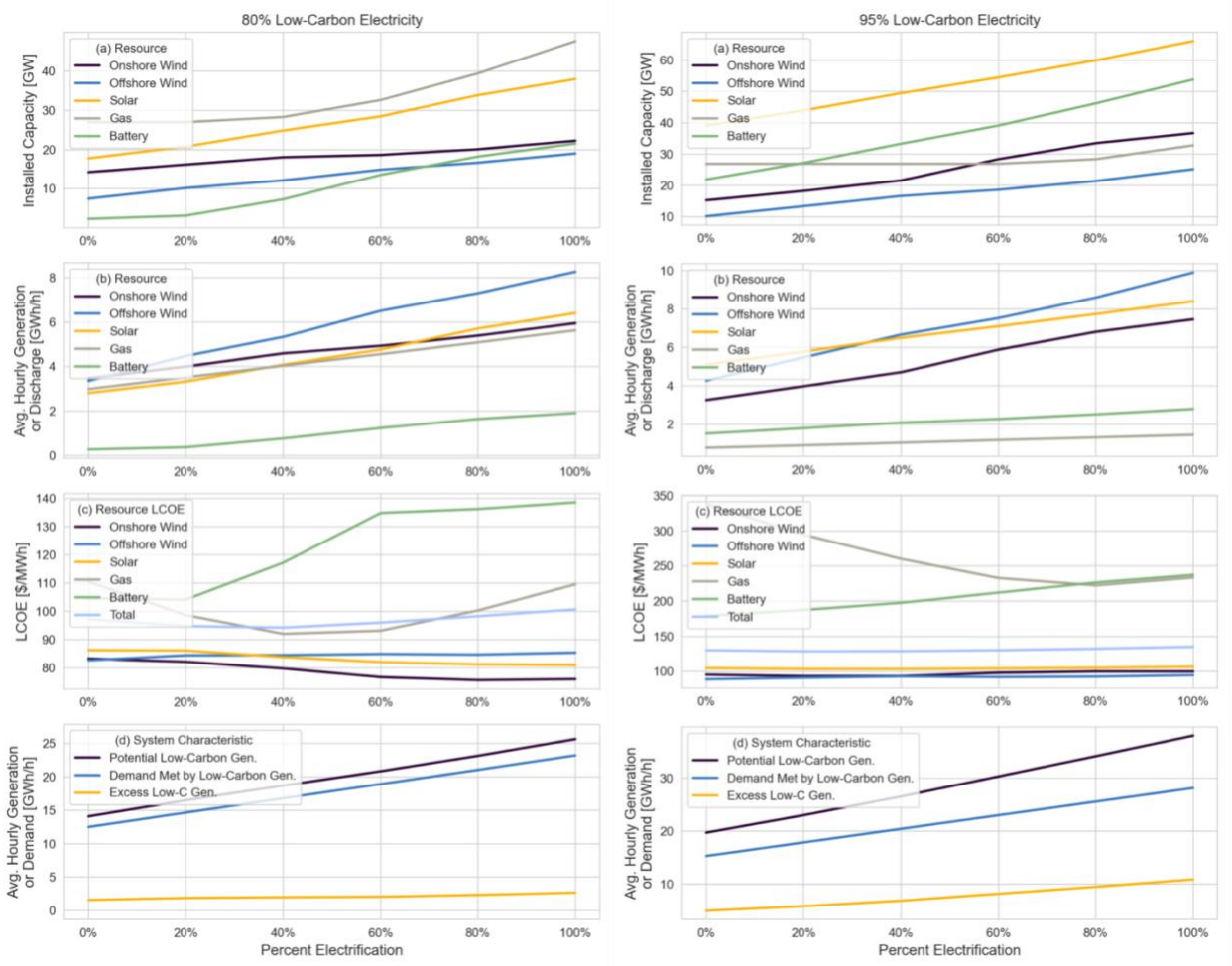

Supplementary Figure S7: System characteristics for scenarios with (a-d) increasing HVE at 80% LCP; and (b) increasing HVE at 95% LCP. Subplots (a, e) present installed capacity; (b, f) present average generation by resource; (c, g) present LCOE per MWh for the generation and storage resources; and (d, h) present demand and generation quantities. In (c, g), resource LCOE for onshore wind, offshore wind, and solar refers to the LCOE of generation; LCOE for battery storage is per-MWh discharge. Note the different y-axis ranges for side-by-side panels.

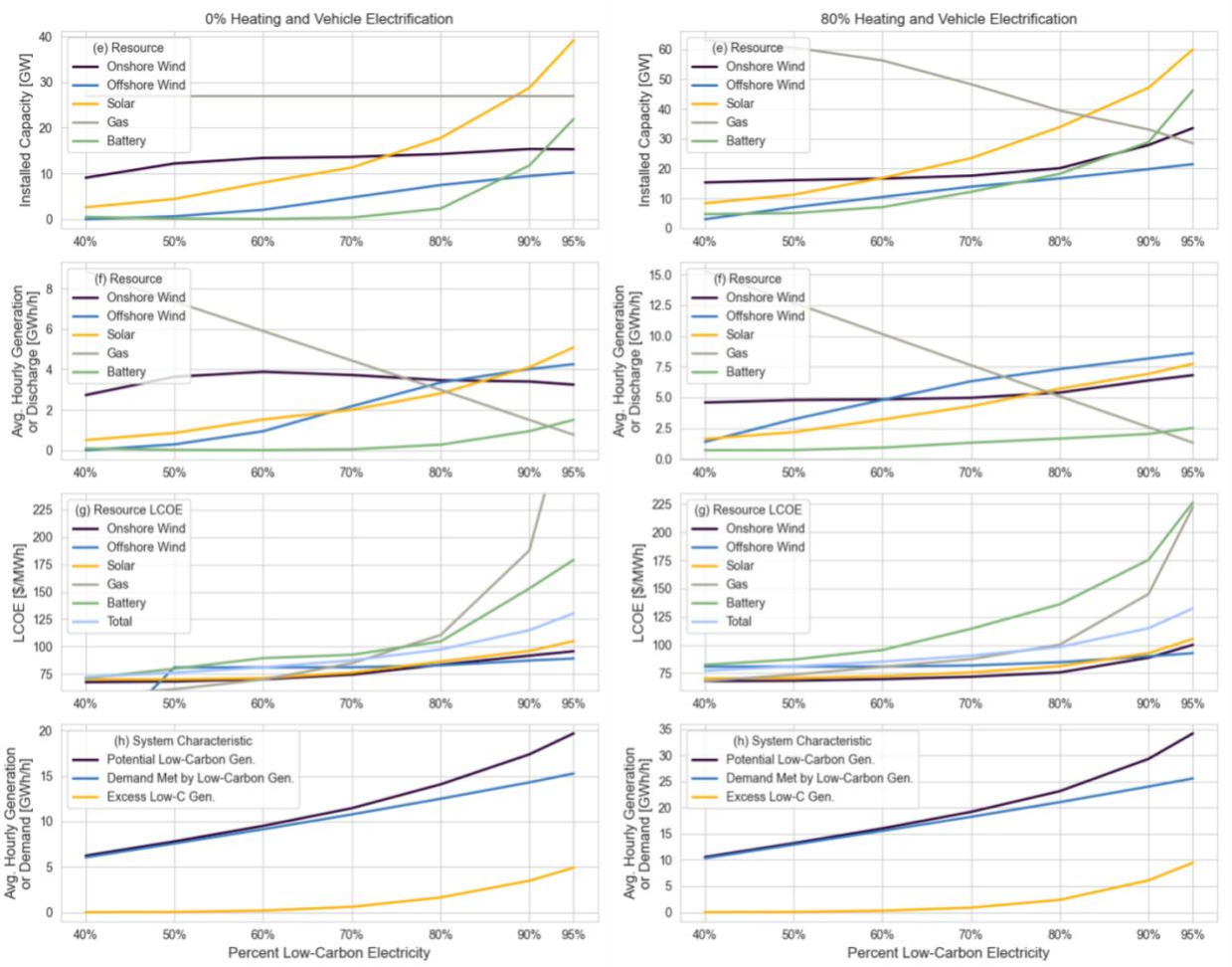

Supplementary Figure S8: System characteristics for scenarios with (a-d) increasing LCP at 0% HVE; and (b) increasing LCP at 80% HVE. Subplots (a, e) present installed capacity; (b, f) present average generation by resource; (c, g) present LCOE per MWh for the generation and storage resources; and (d, h) present demand and generation quantities. In (c, g), resource LCOE for onshore wind, offshore wind, and solar refers to the LCOE of generation; LCOE for battery storage is per-MWh discharge; and in (c), gas generation LCOE at 95% LCP ($338/MWh) is cropped out to preserve y-axis resolution at lower LCOE values. Note the different y-axis ranges for side-by-side panels.

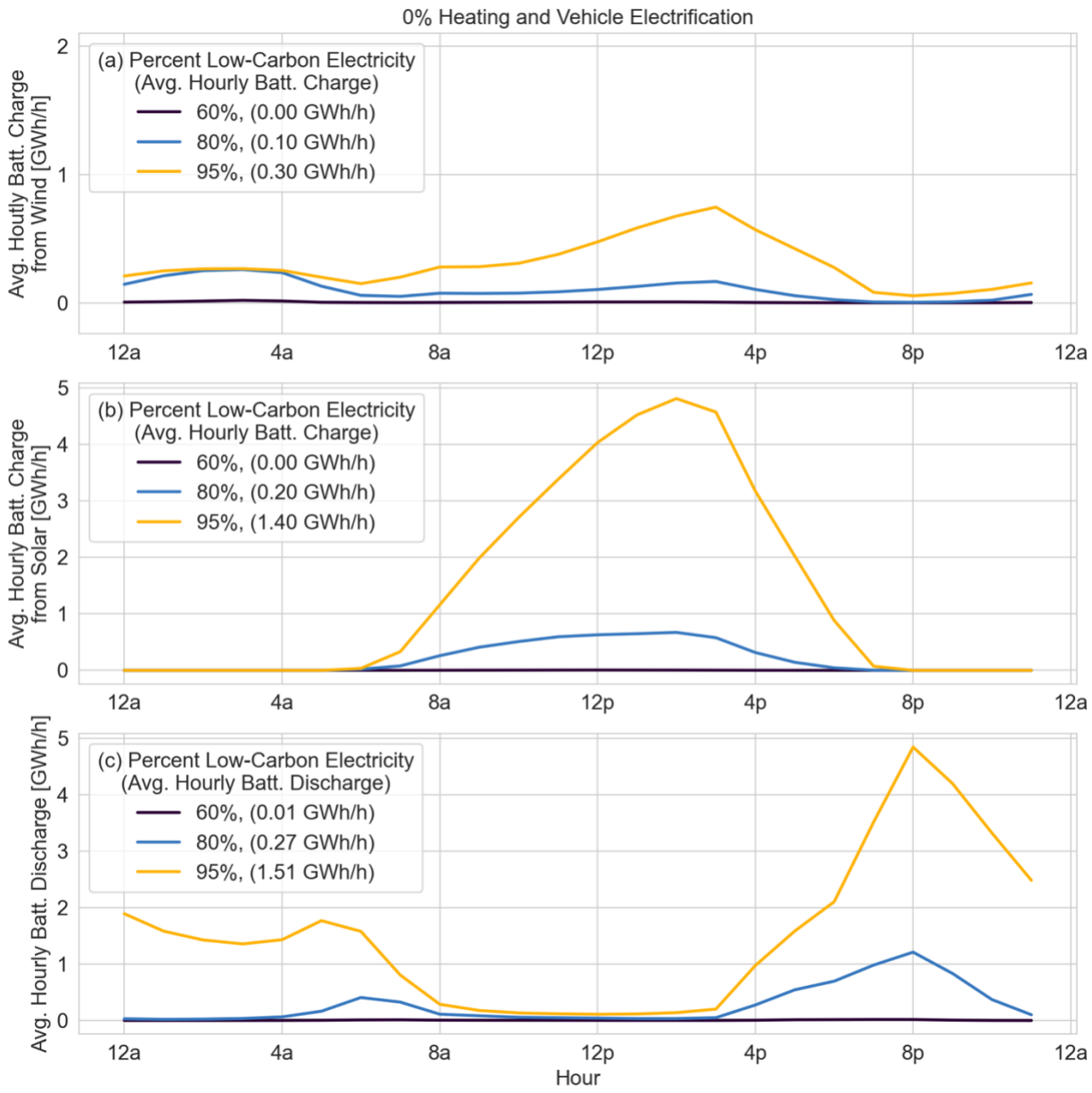

Supplementary Figure S9: *Average battery operation by hour for 60%, 80%, and 95% LCPs at 0% HVE. (a) Average hourly battery charging from wind (note y-axis scale is unique from (b) and (c)); (b) average hourly battery charging from solar; and (c) average battery discharge, all in GWh/h.*

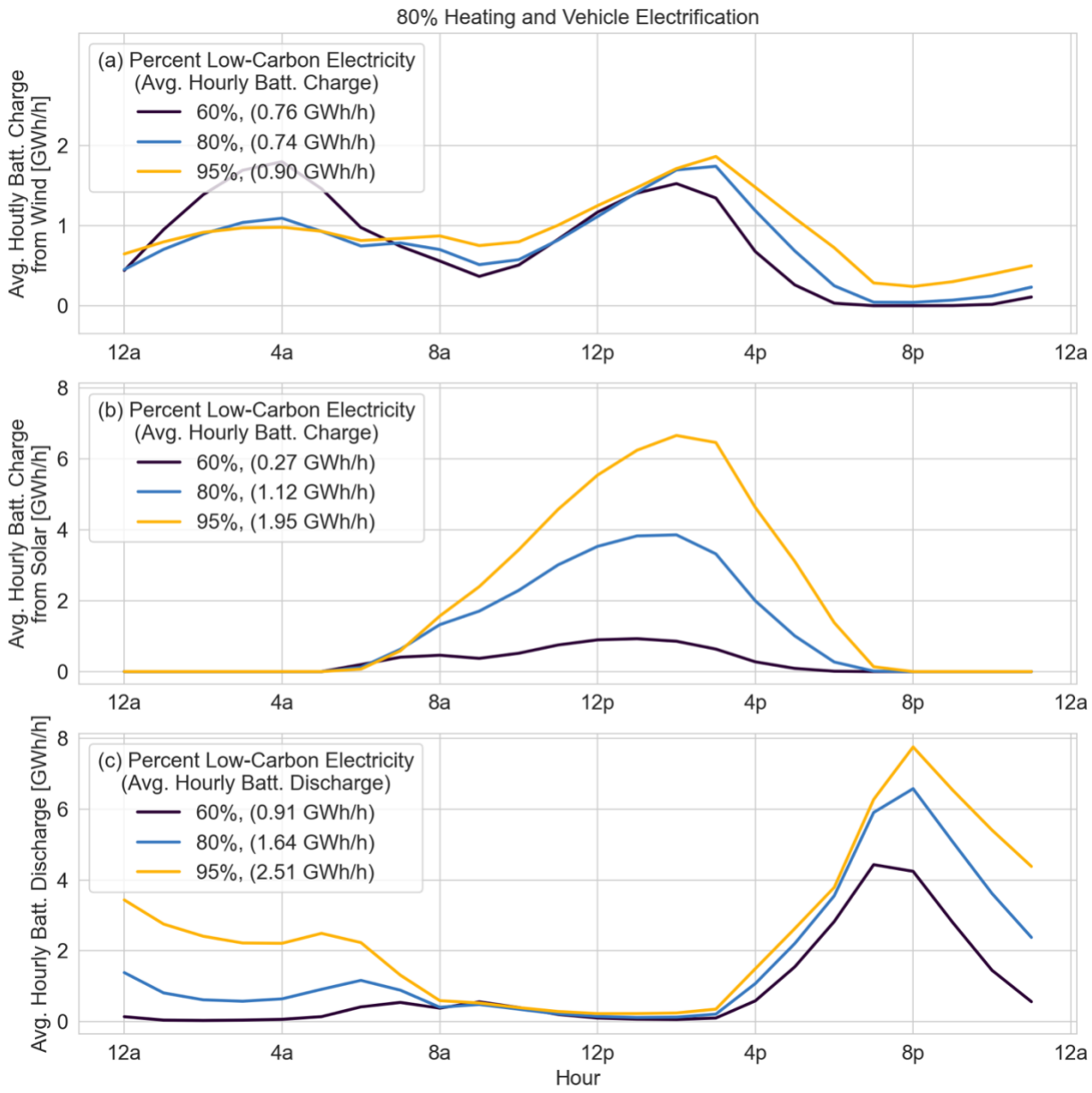

Supplementary Figure S10: *Average battery operation by hour for 60%, 80%, and 95% LCPs at 80% HVE. (a) Average hourly battery charging from wind (note y-axis scale is unique from (b) and (c)); (b) average hourly battery charging from solar; and (c) average battery discharge, all in GWh/h.*

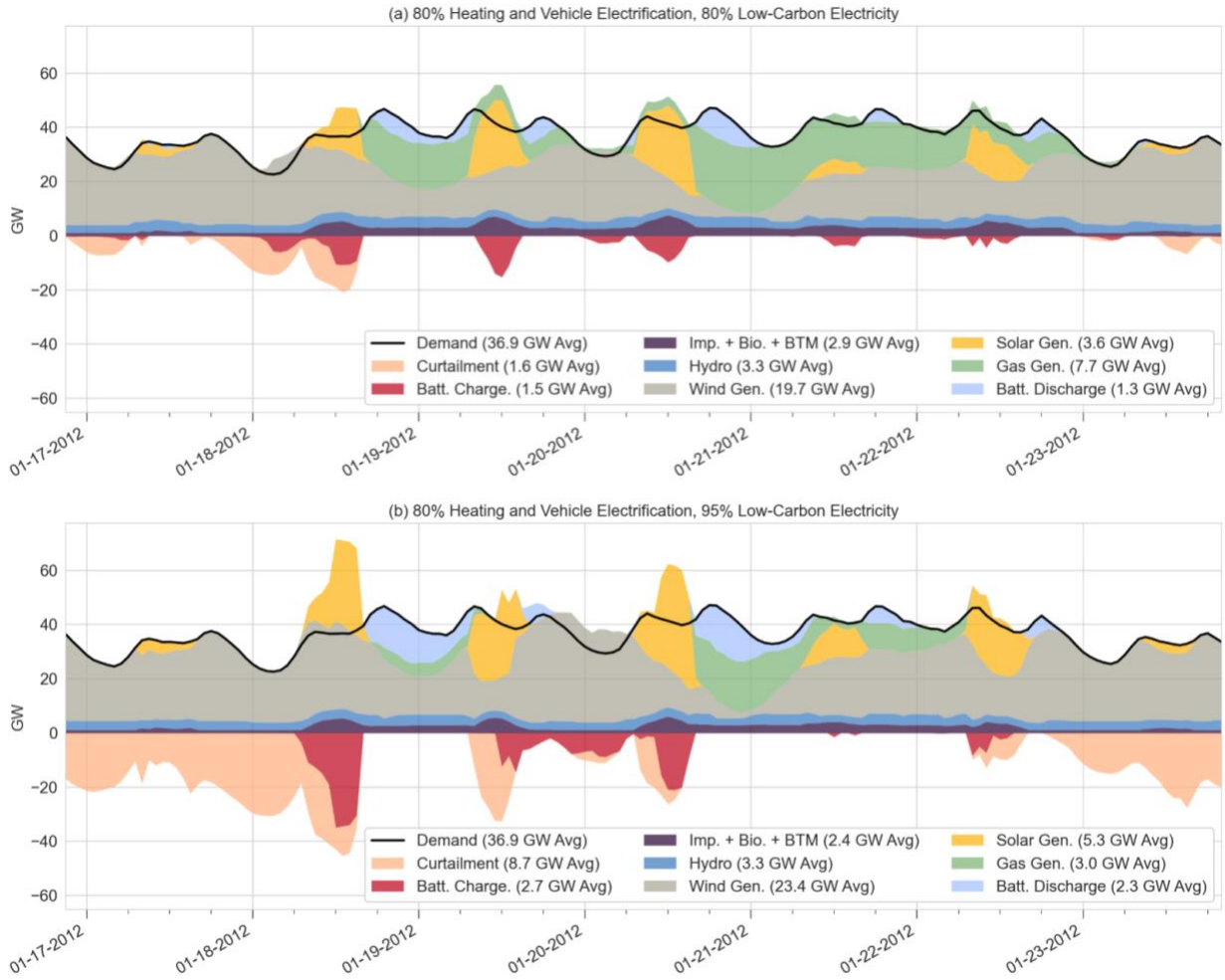

Supplementary Figure S11: Electricity generation and demand for a representative winter week with 80% HVE. (a) 80% LCP; (b) 95% LCP. 'Imp. + Bio. + BTM' represents the sum of imports, biofuel, and behind-the-meter solar generation. Average values reported in the legend are for the week shown.

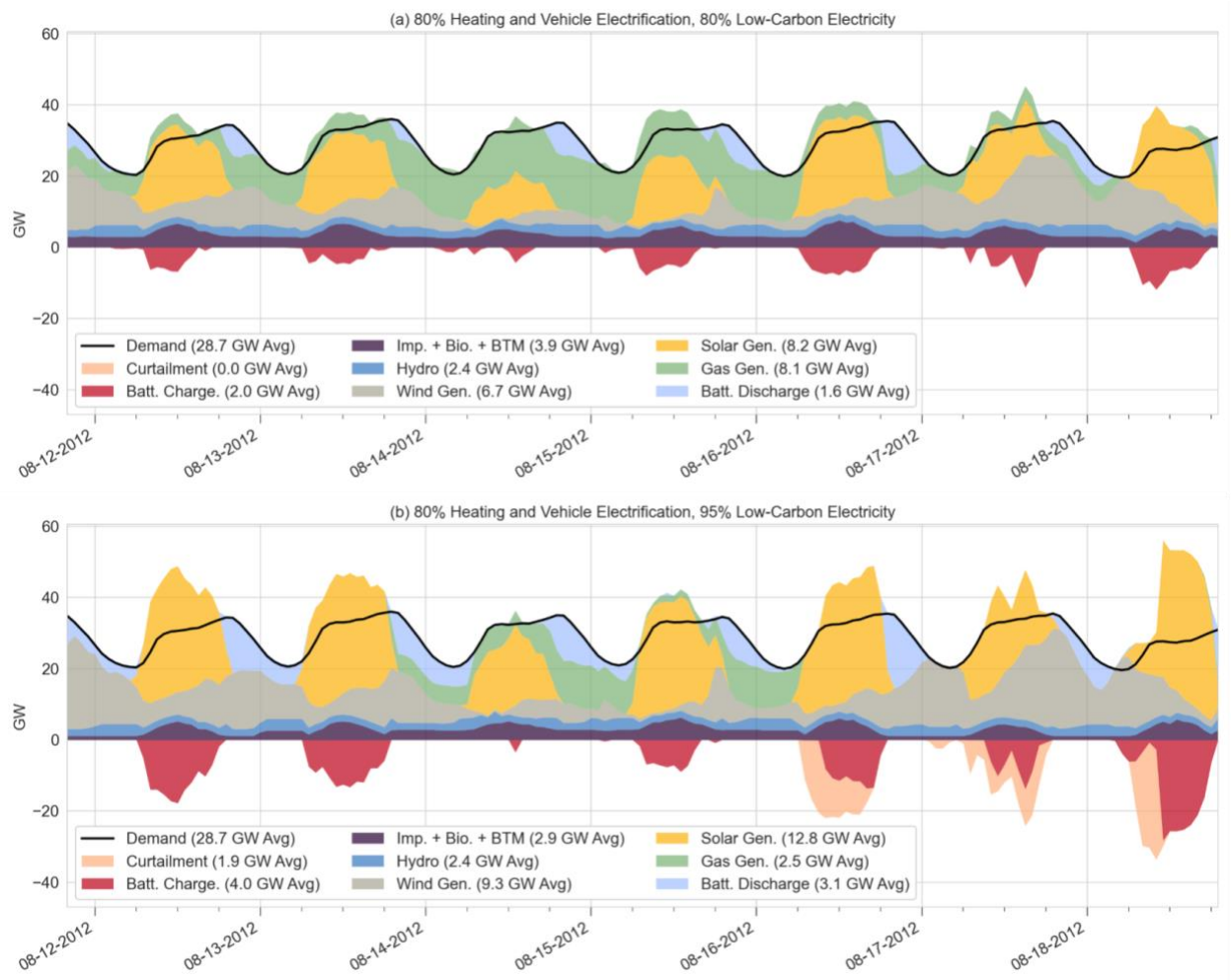

Supplementary Figure S12: Electricity generation and demand for a representative summer week with 80% HVE. (a) 80% LCP; (b) 95% LCP. 'Imp. + Bio. + BTM' represents the sum of imports, biofuel, and behind-the-meter solar generation. Average values reported in the legend are for the week shown.

S4 References

[1] Waite M. Analyses of Energy Infrastructure Serving a Dense Urban Area: Opportunities and Challenges for Wind Power, Building Systems, and Distributed Generation 2016:1–282. https://academiccommons.columbia.edu/doi/10.7916/D8FT8M6H.

[2] US Energy Information Administration (EIA). Cost and Performance Characteristics of New Generating Technologies 2020:1–4. https://www.eia.gov/outlooks/aeo/assumptions/pdf/table_8.2.pdf.

[3] Bloom A, Townsend A, Palchak D, Novacheck J, King J, Barrows C, et al. Eastern Renewable Generation Integration Study 2016:TP-6A20-64. https://www.nrel.gov/grid/ergis.html.

[4] Conlon T, Waite M, Modi V. Assessing new transmission and energy storage in achieving increasing renewable generation targets in a regional grid. Appl Energy 2019;250:1085–98. https://doi.org/10.1016/j.apenergy.2019.05.066.

[5] Opalka W. Appeals Court Ratifies New York Capacity Zone. RTO Insid 2015. https://rtoinsider.com/rto/2d-cir-new-york-ferc-capacity-zone-14255/.

[6] New York Independent System Operator (NYISO). Market and Operational Data 2020. https://www.nyiso.com/energy-market-operational-data.

[7] Waite M, Modi V. Electricity Load Implications of Space Heating Decarbonization Pathways. Joule 2020;4:376–94. https://doi.org/10.1016/j.joule.2019.11.011.

[8] NOAA Centers for Environmental Information. Integrated Surface Dataset 2001. https://www.ncei.noaa.gov/products/land-based-station/integrated-surface-database.

[9] US Energy Information Administration (EIA). Updated Buildings Sector Appliance and Equipment Costs and Efficiencies 2018. https://www.eia.gov/analysis/studies/buildings/equipcosts/.

[10] Northeast Energy Efficiency Partnerships (NEEP). Northeast Energy Efficiency Partnerships Cold Climate Air Source Heat Pump Product Listing 2019. https://ashp.neep.org.

[11] Shapiro C, Puttagunta S. Field Performance of Heat Pump Water Heaters in the Northeast Consortium for Advanced Residential Buildings 2016. https://www.nrel.gov/docs/fy16osti/64904.pdf.

[12] US Energy Information Administration (EIA). State Energy Consumption Estimates 2018. https://www.eia.gov/state/seds/sep_use/notes/use_print.pdf.

[13] US Bureau of Transportation Statistics. Average Age of Automobiles and Trucks in Operation in the United States 2020. https://www.bts.gov/content/average-age-automobiles-and-trucks-operation-united-states.

[14] US Environmental Protection Agency (EPA). The 2020 EPA Automotive Trends Report: Greenhouse Gas Emissions, Fuel Economy, and Technology since 1975 2020:151. https://nepis.epa.gov/Exe/ZyPURL.cgi?Dockey=P1010U68.txt%0A.

[15] New York Open Data. New York State 2016 Gasoline Sales by County 2016. https://data.ny.gov/Energy-Environment/Estimated-Gasoline-Sales-Beginning-1995/cwrk-j5nn.

[16] National Renewable Energy Laboratory (NREL). EVI-Pro Lite API 2021.

https://developer.nrel.gov/docs/transportation/evi-pro-lite-v1/.
[17] New York Independent System Operator (NYISO). New York ISO Reliability Needs Assessment 2020. https://www.nyiso.com/documents/20142/2248793/2020-RNAReport-Nov2020.pdf/64053a7b-194e-17b0-20fb-f2489dec330d.
[18] Goldberg M, Keyser D. Transmission Line Jobs and Economic Development Impact (JEDI) Model User Reference Guide 2016. https://www.nrel.gov/analysis/jedi/transmission-line.html.
[19] MacDonald AE, Clack CTM, Alexander A, Dunbar A, Wilczak J, Xie Y. Future cost-competitive electricity systems and their impact on US CO2 emissions. Nat Clim Chang 2016. https://doi.org/10.1038/nclimate2921.
[20] New York Independent System Operator (NYISO). Western New York Public Policy Transmission Planning Report 2017. https://www.nyiso.com/documents/20142/2892590/Western-New-York-Public-Policy-Transmission-Planning-Report.pdf.
[21] Transmission Developers Inc (TDI). Champlain Hudson Power Express: Project Development Portal 2019. http://ideas.mowerinteractive.com/clients/tdi/60394-website/site/index.php (accessed August 14, 2019).
[22] Starwood Energy Group. The Neptune Regional Transmission System 2007. http://starwoodenergygroup.com/wp-content/uploads/2014/06/6_NeptuneAnnouncement.pdf.
[23] US Energy Information Administration (EIA). Annual Energy Outlook 2020 with projections to 2050 2020. https://www.eia.gov/outlooks/aeo/pdf/aeo2020.pdf.
[24] U.S. Energy Information Administration (EIA). Electric Power Annual 2019 2020. https://www.eia.gov/electricity/annual/.
[25] New York Independent System Operator (NYISO). 2019 Load and Capacity Data: Gold Book 2019. https://www.nyiso.com/documents/20142/2226333/2019-Gold-Book-Final-Public.pdf/.
[26] New York Independent System Operator (NYISO). 2020 Load and Capacity Data: Gold Book 2020. https://www.nyiso.com/documents/20142/2226333/2020-Gold-Book-Final-Public.pdf/.
[27] US Energy Information Administration (EIA). Electric Power Annual Report 2019. Table 5.12. Accessed 10/21/2020. 2020. https://www.eia.gov/electricity/annual/.
[28] US Energy Information Administration (EIA). Electric Power Annual Report 2019. Table 3.11. Accessed 10/21/2020. 2020. https://www.eia.gov/electricity/annual/.
[29] New York Independent System Operator (NYISO). Locational Minimum Installed Capacity Requirements Study for the 2020-2021 Capability Year. 2020. https://www.nyiso.com/documents/20142/8583126/LCR2020-Report.pdf/4c9309b2-b13e-9b99-606a-7af426d93a47.
[30] New York State Energy Research and Development Authority (NYSERDA). New Efficiency: New York Analysis of Residential Heat Pump Potential and Economics 2019. https://www.nyserda.ny.gov/-/media/Files/Publications/PPSER/NYSERDA/18-44-HeatPump.ashx.
[31] Draxl C, Clifton A, Hodge BM, McCaa J. The Wind Integration National Dataset (WIND) Toolkit. Appl Energy 2015;151:355–66. https://doi.org/10.1016/j.apenergy.2015.03.121.

[32] Draxl C, Hodge B-M, Clifton A, McCaa J. Overview and Meteorological Validation of the Wind Integration National Dataset Toolkit. NREL 2015:87. https://www.nrel.gov/docs/fy15osti/61740.pdf.
[33] Waite M, Modi V. Modeling wind power curtailment with increased capacity in a regional electricity grid supplying a dense urban demand. Appl Energy 2016. https://doi.org/10.1016/j.apenergy.2016.08.078.
[34] Musial W, Heimiller D, Beiter P, Scott G, Draxl C. 2016 Offshore Wind Energy Resource Assessment for the United States 2016. https://doi.org/NREL/TP-5000-66599.
[35] Wiser R, Bolinger M, Barbose G, Millstein D. 2016 Wind Technologies Market Report 2017. https://www.energy.gov/eere/wind/downloads/2016-wind-technologies-market-report.
[36] Wiser R, Bolinger M. 2017 Wind Technologies Market Report 2018:1–98. https://www.energy.gov/eere/wind/downloads/2017-wind-technologies-market-report.
[37] Wiser R, Bolinger M. 2018 Wind Technologies Market Report 2019:1–98. https://www.energy.gov/eere/wind/downloads/2018-wind-technologies-market-report.
[38] Wiser R, Jenni K, Seel J, Baker E, Hand M, Lantz E, et al. Expert elicitation survey on future wind energy costs. Nat Energy 2016;1. https://doi.org/10.1038/nenergy.2016.135.
[39] Bloomberg New Energy Finance (BNEF). 2018 Wind O&M Price Index. 2018.
[40] Stehly T, Beiter P, Heimiller D, Scott G, Stehly T, Beiter P, et al. 2017 Cost of Wind Energy Review 2018. https://www.nrel.gov/docs/fy18osti/72167.pdf.
[41] Walter M, Philipp B, Spitsen P, Nunemake J, Gevorgian V. 2018 Offshore Wind Technologies Market Report 2019:1–94. https://www.osti.gov/biblio/1572771-offshore-wind-technologies-market-report.
[42] Bosch J, Staffell I, Hawkes AD. Global levelised cost of electricity from offshore wind. Energy 2019;189:116357. https://doi.org/10.1016/j.energy.2019.116357.
[43] Hummon M, Ibanez E, Brinkman G, Lew D. Sub-Hour Solar Data for Power System Modeling From Static Spatial Variability Analysis. 2nd Int Work Integr Sol Power Power Syst 2012. https://www.nrel.gov/docs/fy13osti/56204.pdf.
[44] Blair N, Dobos AP, Freeman J, Neises T, Wagner M, Ferguson T, et al. System Advisor Model, 2014.1.14: General Description. Natl Renew Energy Lab 2014. http://www.nrel.gov/docs/fy14osti/61019.pdf.
[45] Brooks B, Xenergy K, Whitaker C. Guideline for the use of the Performance Test Protocol for Evaluating Inverters Used in Grid-Connected Photovoltaic Systems. Sandia Natl Lab 2005. https://www.energy.ca.gov/sites/default/files/2020-06/2004-11-22_Sandia_Test_Protocol_ada.pdf.
[46] Fu R, Feldman D, Margolis R. U.S. Solar Photovoltaic System Cost Benchmark: Q1 2018. NREL 2018:1–47. https://doi.org/10.7799/1325002.
[47] USDA National Agricultural Statistics Service. 2017 Census of Agriculture 2017. https://www.nass.usda.gov/Publications/AgCensus/2017/index.php.
[48] Ong S, Campbell C, Denholm P, Margolis R, Heath G. Land-Use Requirements for Solar Power Plants in the United States. 2013. https://doi.org/10.1016/j.rapm.2006.08.004.
[49] NYISO. Solar Impact on Grid Operations: An Initial Assessment 2016:1–57.
[50] New York State Energy Research and Development Authority (NYSERDA). Solar Electric Programs Data (Accessed 06/01/2020) 2020. https://data.ny.gov/Energy-

Environment/Solar-Electric-Programs-Reported-by-NYSERDA-Beginn/3x8r-34rs.
[51] Sengupta M, Habte A, Gotseff P, Weekley A, Lopez A, Molling C, et al. A Physics-Based GOES Satellite Product for Use in NREL's National Solar Radiation Database. Natl Renew Energy Lab 2014. https://www.nrel.gov/docs/fy14osti/62237.pdf.
[52] US Energy Information Administration (EIA). Energy Mapping System 2020. https://www.eia.gov/state/maps.php.
[53] Cole W, Frazier AW. Cost Projections for Utility-Scale Battery Storage: 2020 Update. Natl Renew Energy Lab 2020. https://www.nrel.gov/docs/fy20osti/75385.pdf.
[54] Tesla. Powerpack System Specifications 2019. https://www.tesla.com/powerpack.
[55] Smith K, Saxon A, Keyser M, Lundstrom B, Cao Z, Roc A. Life prediction model for grid-connected Li-ion battery energy storage system. Proc Am Control Conf 2017:4062–8. https://doi.org/10.23919/ACC.2017.7963578.
[56] Aggreko. Aggreko delivers grid stability to New York State with 2MW/3.8MWh energy storage system for National Grid. GlobeNewswire 2019. https://www.globenewswire.com/news-release/2019/06/03/1863350/0/en/Aggreko-delivers-grid-stability-to-New-York-State-with-2MW-3-8MWh-energy-storage-system-for-National-Grid.html.
[57] Lockheed Martin. 1MWh GridStar® Lithium Energy Storage Installation in Syracuse, New York 2019. https://www.lockheedmartin.com/content/dam/lockheed-martin/mfc/documents/energy/energy-syracuses-project-summary.pdf.
[58] Key Capture Energy. KCE NY 1 Breaks Ground on 20 MW 2018. https://www.keycaptureenergy.com/kce-ny-1-breaks-ground-on-20-mw/.
[59] Clean Coalition. Long Island Community Microgrid Project (LICMP) 2019. https://clean-coalition.org/community-microgrids/long-island-community-microgrid-project/.
[60] Energy Storage Association. US Energy Storge: 2019 Year in Review 2019. https://energystorage.org/wp/wp-content/uploads/2020/04/ESA_AR_2020_FINAL.pdf.
[61] Guerra OJ, Zhang J, Eichman J, Denholm P, Kurtz J, Hodge BM. The value of seasonal energy storage technologies for the integration of wind and solar power. Energy Environ Sci 2020;13:1909–22. https://doi.org/10.1039/d0ee00771d.
[62] Steward D, Saur G, Penev M, Ramsden T, Steward D, Saur G, et al. Lifecycle Cost Analysis of Hydrogen Versus Other Technologies for Electrical Energy Storage. Natl Renew Energy Lab 2009. https://www.nrel.gov/docs/fy10osti/46719.pdf.
[63] Houchins C, James B. 2020 DOE Hydrogen and Fuel Cells Program Review 2020. https://www.hydrogen.energy.gov/pdfs/review20/st100_houchins_2020_o.pdf.
[64] Eichman J, Townsend A, Melaina M. Economic Assessment of Hydrogen Technologies Participating in California Electricity Markets. Natl Renew Energy Lab 2016. https://www.nrel.gov/docs/fy16osti/65856.pdf.
[65] Penev M, Rustagi N, Hunter C, Eichman J. Energy Storage: Days of Service Sensitivity Analysis 2019. https://www.nrel.gov/docs/fy19osti/73520.pdf.
[66] Walker SB, Mukherjee U, Fowler M, Elkamel A. Benchmarking and selection of Power-to-Gas utilizing electrolytic hydrogen as an energy storage alternative. Int J Hydrogen Energy 2016;41:7717–31. https://doi.org/10.1016/j.ijhydene.2015.09.008.
[67] Johnson S. New York's Indian Point nuclear power plant closes after 59 years of operation. US Energy Inf Adm Today Energy 2021.

https://www.eia.gov/todayinenergy/detail.php?id=47776#.
[68] New York State Energy Research and Development Authority (NYSERDA). Clean Energy Standard, 2020 Compliance Year: Load Serving Entity (LSE) Zero Emission Credit (ZEC) Rate. 2020. https://www.nyserda.ny.gov/All-Programs/Clean-Energy-Standard/LSE-Obligations/2020-Compliance-Year.
[69] US Energy Information Administration (EIA). Form EIA-923 detailed data with previous form data (EIA-906/920) 2020. https://www.eia.gov/electricity/data/eia923/.
[70] Mukerji R. NYISO Market Operations Report. New York Indep Syst Oper 2019. https://www.nyiso.com/documents/20142/8196990/Market+Operations+Report_+BIC_09.11.19.pdf.
[71] Whitney N. Amount of Capacity Qualified to Offer. New York Indep Syst Oper 2019. nyiso.com/documents/20142/3036383/4_Amt of Capacity Qualified to Offer.pdf/57f56a99-3293-d795-8584-21a70c495a5a.
[72] New York City Council. Local Laws of the City of New York for the Year 2019. No. 97. 2019. https://www1.nyc.gov/assets/buildings/local_laws/ll97of2019.pdf.
[73] NYSERDA. New York State Greenhouse Gas Inventory: 1990-2016 2019. https://www.nyserda.ny.gov/-/media/Files/EDPPP/Energy-Prices/Energy-Statistics/greenhouse-gas-inventory.pdf.
[74] New York State Senate. Climate Leadership and Community Protection Act — Final Bill Text 2019. https://www.nysenate.gov/legislation/bills/2019/s6599.
[75] Myrhe G, Shindell D, Huang J, Mendoza B, Daniel JS, Nielsen CJ, et al. Anthropogenic and natural radiative forcing. Clim Chang 2013 Phys Sci Basis Work Gr I Contrib to Fifth Assess Rep Intergov Panel Clim Chang 2013;9781107057:659–740. https://doi.org/10.1017/CBO9781107415324.018.
[76] Howarth RW. Methane Emissions and Greenhouse Gas Accounting: A Case Study of a New Approach Pioneered by the State of New York 2019:14. https://documents.dps.ny.gov/public/Common/ViewDoc.aspx?DocRefId=%7B3498AB82-B671-451E-A556-A917A61F939A%7D.
[77] Hayhoe K, Kheshgi HS, Jain AK, Wuebbles DJ. Substitution of natural gas for coal: Climatic effects of utility sector emissions. Clim Change 2002;54:107–39. https://doi.org/10.1023/A:1015737505552.
[78] Howarth RW, Santoro R, Ingraffea A. Methane and the greenhouse-gas footprint of natural gas from shale formations. Clim Change 2011;106:679–90. https://doi.org/10.1007/s10584-011-0061-5.
[79] Intergovernmental Panel on Climate Change (IPCC). Good Practice Guidance and Uncertainty Management in National Greenhouse Gas Inventories. Table 2, CH4 Emissions: Coal Mining and Handling. 1996. https://www.ipcc-nggip.iges.or.jp/public/gp/english/.
[80] National Energy Technology Laboratory (NETL). Petroleum-Based Fuel Life Cycle Greenhouse Gas Analysis - 2005 Baseline Model 2008. https://www.nata.aero/data/files/gia/environmental/bllcghg2005.pdf.
[81] Alvarez RA, Zavala-Araiza D, Lyon DR, Allen DT, Barkley ZR, Brandt AR, et al. Assessment of methane emissions from the U.S. oil and gas supply chain. Science (80-) 2018;361:186–8. https://doi.org/10.1126/science.aar7204.

[82] Schneising O, Burrows JP, Dickerson RR, Buchwitz M, Reuter M, Bovensmann H. Remote sensing of fugitive methane emissions from oil and gas production in North American tight geologic formations. Earth's Futur 2014;2:548–58. https://doi.org/10.1002/2014ef000265.
[83] Engineering ToolBox. Fuels - Higher and Lower Calorific Values 2003. https://www.engineeringtoolbox.com/fuels-higher-calorific-values-d_169.html.
[84] EPA. Emission Factors for Greenhouse Gas Inventories 2019:1–5. https://www.ecfr.gov/current/title-40/chapter-I/subchapter-C/part-98#ap40.23.98_19.1.
[85] Hydro-Quebec. Hydro Quebec Annual Report 2019 2020. https://www.hydroquebec.com/data/documents-donnees/pdf/annual-report.pdf.